

## Gastrointestinal imaging-practical magnetic resonance imaging approach

Baodong Liu, Miguel Ramalho, Mamdoh AIObaidy, Kiran K Busireddy, Ersan Altun, Janaka Kalubowila, Richard C Semelka

Baodong Liu, Miguel Ramalho, Mamdoh AIObaidy, Kiran K Busireddy, Ersan Altun, Janaka Kalubowila, Richard C Semelka, Department of Radiology, University of North Carolina at Chapel Hill, North Carolina, NC 27599-7510, United States  
Author contributions: Liu B, Ramalho M, AIObaidy M, Busireddy KK, Altun E, Kalubowila J and Semelka RC equally contributed to this work; including literature review, manuscript writing, manuscript editing, figures collection and writing figures captions.

Correspondence to: Richard C Semelka, MD, Department of Radiology, University of North Carolina at Chapel Hill, 2001 Old Clinic Bldg., CB 7510, Chapel Hill, North Carolina, NC 27599-7510, United States. richsem@med.unc.edu

Telephone: +1-919-9669676 Fax: +1-919-8437147

Received: February 11, 2014 Revised: April 15, 2014

Accepted: May 31, 2014

Published online: August 28, 2014

### Abstract

Over the past two decades, advances in cross-sectional imaging such as computed tomography and magnetic resonance imaging (MRI) have dramatically changed the concept of gastrointestinal imaging. MR is playing an increasing role in the evaluation of gastrointestinal disorders. MRI combines the advantages of excellent soft-tissue contrast, noninvasiveness, functional information and lack of ionizing radiation. Furthermore, recent developments of MRI have led to improved spatial and temporal resolution as well as decreased motion artifacts. In this article we describe the technical aspects of gastrointestinal MRI and present a practical approach for a well-known spectrum of gastrointestinal disease processes.

© 2014 Baishideng Publishing Group Inc. All rights reserved.

**Key words:** Magnetic resonance imaging; Crohn's disease; Celiac disease; Appendicitis; Diverticulitis; Rectal cancer; Gastric tumors; Small bowel tumors

**Core tip:** The implementation of fast and ultra-fast sequences and dedicated advanced imaging protocols render magnetic resonance imaging (MRI) an excellent tool for gastrointestinal (GI) imaging. State of the art MRI/magnetic resonance enterography has rapidly emerged as successful gastrointestinal imaging modality, offering detailed anatomic and morphologic information and also permitting evaluation of extra-luminal manifestation and extension of disease. The lack of ionizing radiation makes MRI the preferred modality in many GI disease processes. In this article we describe the technical aspects of gastrointestinal MRI and present a practical approach for a well-known spectrum of gastrointestinal disease processes.

Liu B, Ramalho M, AIObaidy M, Busireddy KK, Altun E, Kalubowila J, Semelka RC. Gastrointestinal imaging-practical magnetic resonance imaging approach. *World J Radiol* 2014; 6(8): 544-566 Available from: URL: <http://www.wjgnet.com/1949-8470/full/v6/i8/544.htm> DOI: <http://dx.doi.org/10.4329/wjr.v6.i8.544>

### INTRODUCTION

Medical imaging of the gastrointestinal (GI) tract is crucial for the diagnosis of GI diseases. Historically, barium techniques have been the only available method. Although many diagnoses have been made on the basis of these exams, the diagnostic performance of these exams for certain abnormalities has been disappointing<sup>[1]</sup>.

Over the past two decades, advances in cross-sectional imaging such as computed tomography (CT) and magnetic resonance imaging (MRI) have dramatically changed the concept of GI imaging. Recently, developments in endoscopic techniques, especially the advent of capsule

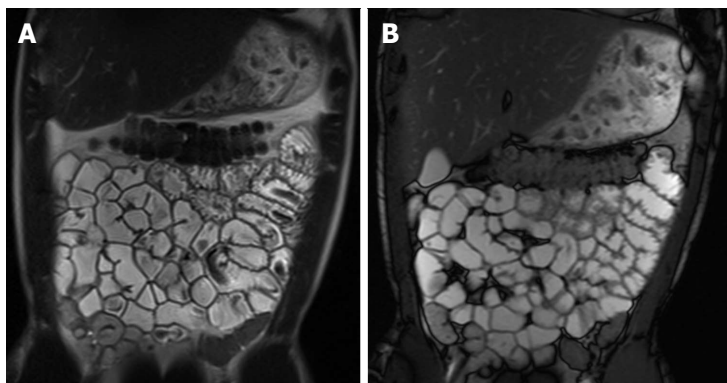


**Figure 1** Coronal T2-weighted single shot fast spin echo and coronal balanced steady state free precession images. Good bowel distension is achieved with the administration of peroral fluid (A and B). Balanced steady state free precession sequence (B) is robust to flow voids; in addition to its ability to demonstrate fine anatomical details including bowel thickness, mesenteric vessels and lymph nodes; even without the use of spasmolytic agents.

endoscopy (CE) have made it possible to provide direct mucosal visualization of the GI tract. However, CE also has such limitations in disease localization, and is contraindicated in patients with suspected of bowel stricture or obstruction<sup>[1,2]</sup>.

MR and CT techniques optimized for small bowel imaging are playing an increasing role in the evaluation of gastrointestinal disorders. Several studies have shown the advantage of these techniques over traditional barium fluoroscopic examinations. Cross-sectional techniques have several advantages, including their ability to display the entire thickness of the gastric and bowel wall, visualize the deep pelvis ileal loops without superimposition, and evaluate the mesentery and perienteric fat. Another intrinsic advantage is the possibility to assess solid organs and provide a global overview of the abdominopelvic cavity.

The preference of MR over CT is mainly based on available resources and public policies. However, similar to fluoroscopic procedures, CT is associated with patients' radiation exposure. With the increasing awareness of radiation exposure, there has been a more global interest in implementing techniques that either reduce or eliminate radiation exposure<sup>[3]</sup>. This may be of particular importance in radiosensitive patient population with chronic inflammatory bowel disease; who may require multiple studies over a lifetime<sup>[4]</sup>. As a result, MRI has become increasingly important as a method of evaluating various gastrointestinal disease processes<sup>[5]</sup>.

MRI combines the advantages of excellent soft-tissue contrast, noninvasiveness, functional information and lack of ionizing radiation. Furthermore, recent developments of MRI have led to improved spatial and temporal resolution as well as decreased motion artifacts<sup>[6]</sup>. In this article we describe technical aspects of gastrointestinal MRI and present a practical approach for a well-known spectrum of gastrointestinal disease processes.

## PRACTICAL ASPECTS OF GASTROINTESTINAL MRI TECHNIQUE

Similar to other imaging techniques, adequate luminal

distension is desirable since poorly distended loops can simulate<sup>[7]</sup> or hide pathologic processes; especially in less experienced hands. Two different techniques to provide sufficient luminal distension of the small bowel have been proposed: MR enteroclysis and MR enterography. MR enteroclysis is associated with excellent image quality because of superb bowel distension achieved by fluid administration after nasojejunal intubation. However, the placement of the catheter is unpleasant and stressful for the patient. The improved distention achieved with enteroclysis does not necessarily translate into an improvement in diagnostic effectiveness<sup>[8,9]</sup> and peroral fluid administration results in effective and most often satisfactory means of achieving small bowel distention. One advantage of MR enteroclysis may reside in the detection of mesenteric small bowel tumors<sup>[10,11]</sup>.

Three groups of contrast agents can be utilized to achieve distension and are classified as positive (bright lumen), negative (dark lumen), or biphasic contrast agents. Biphasic contrast agents (water-based) are usually preferred because they are easy to implement and provide excellent signal characteristics, resulting in bright lumen on T2-weighted and dark lumen on T1-weighted sequences. Tap water is frequently used as a biphasic contrast agent, especially when imaging the upper gastrointestinal segment (stomach, duodenum and proximal jejunum); however, it is rapidly reabsorbed in the small intestine, leading to a poor distension of the distal jejunum and ileum. In order to slow intestinal absorption of water, higher-osmolality and viscosity agents are routinely added<sup>[12-14]</sup>. After a 4 to 6-h fast, patients are asked to drink between 1000 mL and 1500 mL of intraluminal contrast (Figure 1); 45 to 55 min prior to examination. Metoclopramide (20 mg) may be added directly to the oral contrast to promote gastric emptying. Adverse effects are rare, usually mild and transitory, and experienced mainly after the termination of the MR examination<sup>[15]</sup>.

Some patients cannot tolerate the ingestion of high volumes of oral contrast; in our experience, we found that luminal distension is not as critical as on CT and the MR examination can still be performed even if only a

small volume has been ingested.

Patients undergoing magnetic resonance enterography (MRE) should be examined in prone position. This position may facilitate separation of small bowel loops while decreasing the volume of peritoneal cavity to be imaged, and, as a result, the number of coronal sections to be acquired<sup>[16]</sup>. Hence, acquisition times and consequently the time span for breath holding can be decreased. However, many patients may not tolerate lying prone in the MR scanner, and therefore supine position is almost always adequate.

Gastrointestinal MR evaluation is based on the ultra-fast imaging generally applied for body MRI. Body MRI is still based on T1-weighted and T2-weighted sequences plus or minus fat-suppression and postgadolinium T1-weighted sequences. A combination of single-shot fast/turbo spin-echo T2-weighted and gradient recalled echo (GRE) T1-weighted sequences with intravenous gadolinium enhancement and fat-suppression result in consistent image quality of the gastrointestinal tract. Two- or three-dimensional balanced steady-state free precession (bSSFP) sequences are additionally collected as part of the MRE protocol.

Single-Shot turbo spin echo (TSE)/FSE T2-weighted sequences are very robust to motion and usually acquired with and without fat-saturation. These sequences have high sensitivity for fluid and are crucial to depict edema in or adjacent to the bowel wall. This is especially important in Crohn's disease (CD), which can be regarded as a marker for active inflammation. Single-shot sequences are susceptible to flow artifacts, and thus intraluminal flow voids can be seen (Figure 1).

Because bSSFP sequences are relatively robust with regard to motion artifacts and intraluminal flow voids, these sequences are performed in the beginning of the study prior to glucagon or intravenous contrast administration. These sequences can be performed quickly and are complementary to single-shot TSE/FSE sequences and the preferred pulse sequence to evaluate the mesentery. The ratio of T1/T2 contrast provides images that appear primarily T2-weighted, with very high signal for all types of fluid. This feature allows good evaluation of the bowel wall, particularly in the definition of edema and of bowel wall layering appearance. Cine-analysis can also be performed with this technique allowing supplementary functional information. We generally acquire 15-25 frames per section location during free breathing. These images may then be displayed as a cine loop to assess bowel motility to exclude or confirm fixed stenoses, segmental dilatation, and detect adhesions.

T1-weighted GRE MRI represents the core of the body MR protocol. Since these sequences are quite prone to bowel motion artifacts, spasmolytic agents (*e.g.*, Glucagon<sup>®</sup> or Buscopan<sup>®</sup>) should be administered intravenously immediately before image acquisition. Buscopan<sup>®</sup> is less expensive; however, it is not Food and Drug Administration approved and therefore not available in the United States. These sequences are performed as either 2D or 3D techniques, and on newer MR sys-

tems, the most commonly used is the 3D-GRE with fat-suppression. Post-contrast coronal and axial images are also acquired. Our protocol includes an arterial and interstitial phase in the coronal plane and an enteric (early hepatic-venous) phase (circa 50 s) in the axial plane. Gadolinium-enhanced T1-weighted images are helpful to detect both intestinal tumors and inflammatory bowel diseases with high sensitivity<sup>[17]</sup>.

Diffusion-weighted imaging (DWI) has been increasingly used for body MRI. Initial studies underline a possible value of DWI also for small bowel imaging, aiding in the assessment of disease activity<sup>[18,19]</sup>. A set of coronal diffusion-weighted images ( $b = 0-50 \text{ s/mm}^2$ ;  $b = 600-800 \text{ s/mm}^2$ ) may be added to the protocol, depending on the indication of the examination and preference of the radiologist. This is especially important in pregnant patients those with contraindications to gadolinium administration (Figure 2).

---

## PRACTICAL APPROACH TO INFLAMMATORY CONDITIONS-SMALL BOWEL

---

### CD

CD is a chronic relapsing inflammatory disease of the gastrointestinal tract involving all layers of the bowel wall and may be classified as active inflammatory (without fistulas or strictures), penetrating, or fibrostenotic disease<sup>[20]</sup>. Although any segment of the gastrointestinal tract may be involved with CD, it most commonly involves the terminal ileum, and frequently in association with disease in the right colon.

Endoscopy and histologic examination have served as the standard approach for the diagnosis of CD; however, diagnosing lesions in the small bowel between the distal duodenum and mid ileum has been a challenge. Furthermore, the major disadvantage of endoscopic methods endoscopic tests and biopsies will evaluate the mucosa but do not evaluate inflammation or fibrosis within the submucosa or deeper tissues. Currently, CT enterography and MRE are the only two imaging modalities that enable the visualization of submucosal tissues throughout the entire small bowel; however, as stated above, MRE does not expose patients to ionizing radiation and it provides additional technical and diagnostic advantages<sup>[21]</sup>.

The following important questions can be addressed on MRE: (1) extent of small and large bowel involvement; (2) distinction between active inflammatory and fibrotic stricturing disease; (3) recognition of penetrating disease  $\pm$  extramural complications; (4) evaluation of response to medical therapy; and (5) detection of recurrent disease following surgery.

A relatively simple and accurate approach for evaluation of CD activity is based on the association of T2-weighted and post-gadolinium T1-weighted sequences. This combination allows comprehensive evaluation and discrimination between quiescent disease and active inflammation and for evaluation of complications includ-

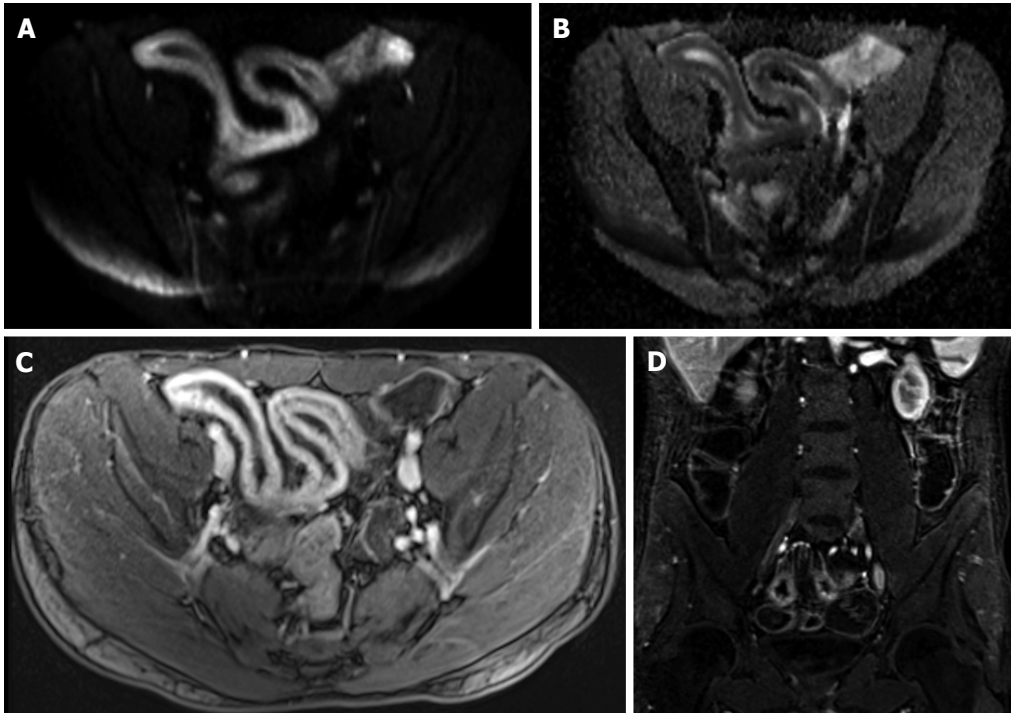


**Figure 2 Active distal ileal Crohn's disease.** Axial diffusion weighted imaging (A) ( $b = 150$ ) and (B) apparent diffusion coefficient map as well as (C) axial and (D) coronal fat-suppressed post-gadolinium 3D-GRE T1-weighted images. There is a long segment of distal ileal diffuse thickening associated with diffusion restriction (A and B) as well as significant contrast enhancement (C) and vasa recta engorgement (comb sign) (D) in keeping with active Crohn's disease. GRE: Gradient recalled echo.

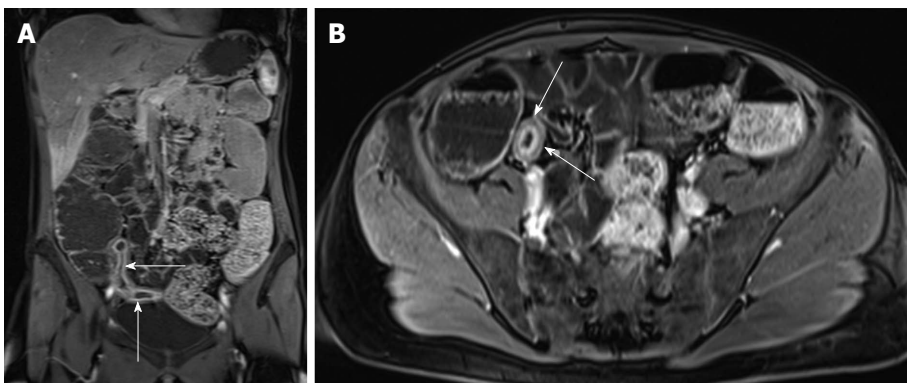


**Figure 3 Enhancement of bowel wall layers in active Crohn's disease.** Coronal (A) and (B) axial fat-suppressed post-gadolinium 3D-GRE T1-weighted images during the (A) arterial and (B) enteric phase in a patient with active Crohn's disease. There is extensive mucosal enhancement involving the affected terminal ileum (arrows, A), reflecting active disease. Enteric phase images (B) shows serosal enhancement providing the tri-laminar appearance of active disease (arrows, B). GRE: Gradient recalled echo.

ing abscesses or fistulas<sup>[21,22]</sup>.

#### **Findings perceived on post-gadolinium T1-weighted images**

Increased mucosal enhancement has long been one of the most important findings and is the most sensitive finding of disease activity, which may approach 100% sensitivity<sup>[23-27]</sup>. Imaging findings of mucosal enhancement; bowel wall edematous thickening ( $> 3$  mm); and enhancement of different bowel layers, termed "mural stratification", are classic features of active small bowel disease<sup>[28,29]</sup> (Figure 3). Quantitative bowel enhancement parameters were found to correlate highly with histologic and endoscopic disease severity<sup>[30]</sup>.

Other findings include stranding extending into the mesenteric border fat and engorgement of the hyperemic vasa recta surrounding the inflamed bowel segment (comb sign) and reactively enlarged and hyper-enhancing mesenteric lymph nodes.

#### **Perceived on T2-weighted images**

Bowel wall thickening with increased T2-signal within or adjacent to the abnormal bowel on fat-suppressed images indicates active inflammation<sup>[31]</sup>. Other signs include fluid accumulation in adjacent intraperitoneal and mesenteric spaces (Figure 4).

Fibrofatty proliferation or creeping of the mesenteric fat along the mesentery and onto the involved bowel seg-

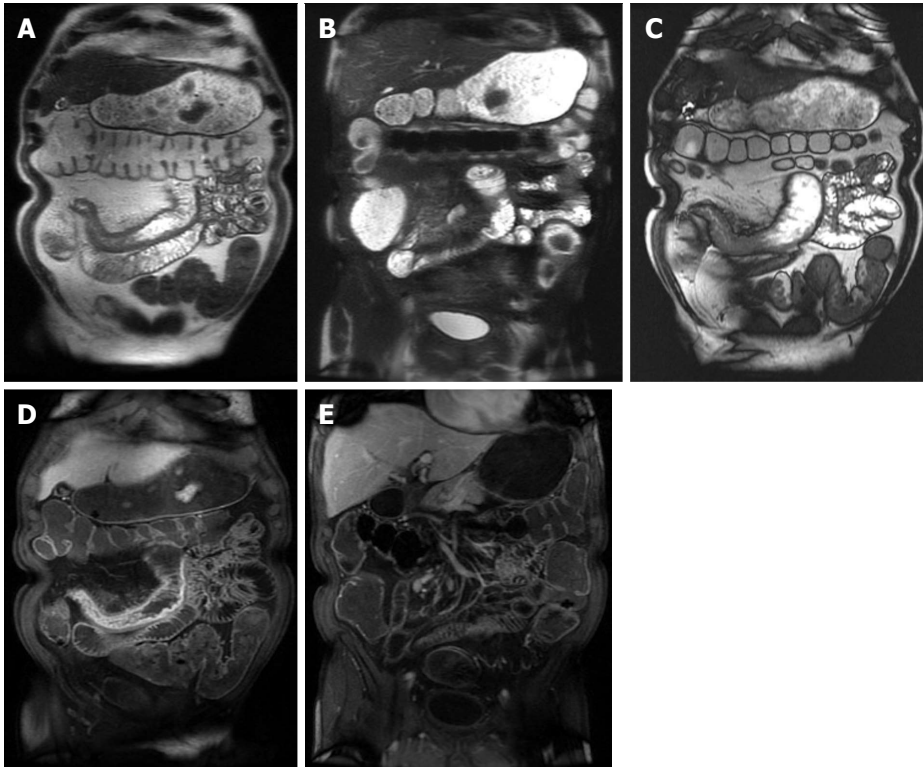


**Figure 4 Active Crohn's disease.** A and B: Coronal T2-weighted single shot fast spin echo without and with fat suppression and © coronal balanced steady state free precession image as well as coronal fat-suppressed post-gadolinium 3D-GRE T1-weighted images during the (D) arterial and E: interstitial phases. There is abnormal bowel wall thickening and edema involving distal ileal segments, associated with small fluid collection in the adjacent mesentery (A and B), engorgement of the mesenteric vessels (comb sign) (C-E), and extensive mucosal enhancement (D and E), in addition to the presence of enhancing mesenteric lymph nodes, in keeping with active Crohn's disease.

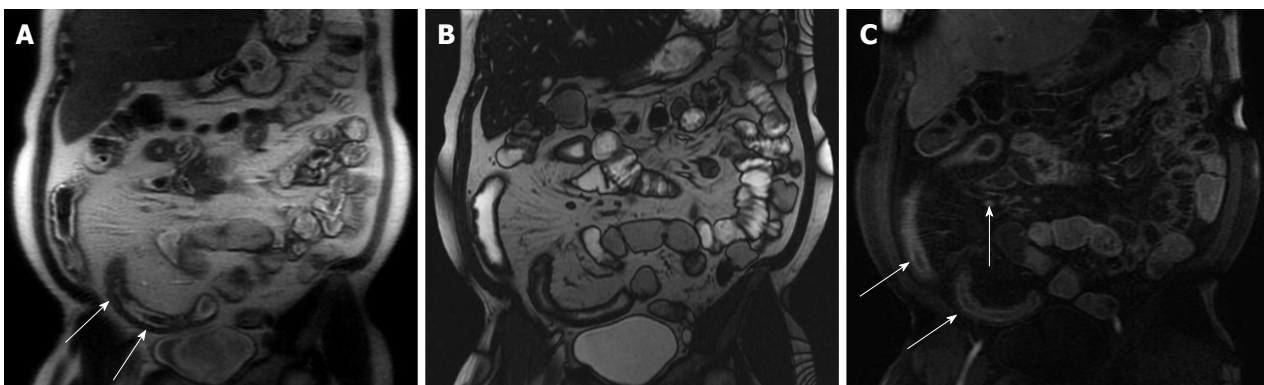


**Figure 5 Active Crohn's disease.** A: Coronal T2-weighted single shot fast spin echo and (B) coronal balanced steady state free precession (bSSFP) images as well as (C) coronal fat-suppressed post-gadolinium 3D-GRE T1-weighted images during the interstitial phase. There is an abnormal segment of distal ileal thickening with diffuse submucosal increased T2 signal intensity (arrows, A) displaying high signal intensity, consistent with edema. The bSSFP image (B) doesn't demonstrate submucosal edema, but clearly depicts mesenteric lymph nodes and comb sign, associated with extensive mucosal enhancement (arrows, C), reflecting disease activity. Fibrofatty proliferation around the affected ileal segments is also seen. GRE: Gradient recalled echo.

ment (Figure 5) suggests a chronically inflamed bowel loop, a sign mostly seen in chronic disease. However, when it is associated with engorged perpendicular distal mesenteric vessels (comb sign), it is considered surgically pathognomonic for the disease and highly specific for active CD<sup>[32]</sup>. Comb sign is usually well depicted on bSSFP sequences (Figure 5).

**Practical interpretive approach to a thickened bowel wall segment**

**Active inflammation:** Bowel wall thickening and en-

hancement on post-gadolinium T1-weighted images, plus high signal intensity on T2-weighted fat-suppressed images<sup>[21]</sup> (Figures 4 and 5).

**Chronic disease without active inflammation:** Bowel wall thickening and reduced and homogeneous enhancement on post-gadolinium T1-weighted images without a layering enhancement; plus low T2-signal intensity on fat-suppressed images with possible stenosis with obstruction and occasionally sacculations or dilated amorphous bowel loops. In the fibrostenotic disease subtype, MRE



**Figure 6 Chronic Crohn's disease.** A: Coronal T2-weighted single shot fast spin echo and (B) coronal balanced steady state free precession (bSSFP), images as well as coronal fat-suppressed post-gadolinium 3D-GRE T1-weighted images during the (C) arterial and (D) interstitial phases. There is an intermediately low T2 signal intensity bowel wall thickening involving the distal ileum (A), also well-appreciated on bSSFP image (B), showing negligible enhancement on post-gadolinium images (arrows, C and D), consistent with chronic fibrotic segment without superimposed inflammation. A pre-stenotic dilatation is observed. GRE: Gradient recalled echo.

demonstrates a fixed narrowing of the involved bowel with associated wall thickening and marked pre-stenotic dilatation<sup>[21]</sup>. On MRE cine imaging, fibrotic strictures appear as aperistaltic bowel segment that often demonstrate fixed mural thickening and luminal narrowing; these sequences help to differentiate a fibrotic stricture from small bowel obstruction secondary to spasm associated with active inflammatory disease<sup>[33]</sup> (Figure 6).

**Chronic disease with active inflammation:** These features can overlap with active inflammation and sometimes only distinguished upon further short-term follow-up post-trial medical treatment. Acute on chronic involvement is suggested by marked enhancement of the mucosa with substantial low T2 signal intensity and minimal enhancement of the outer layer; therefore, appreciation of these findings may have a role in the evaluation of acute exacerbations of CD. The presence of sub-mucosal intramural fat deposition, which is also related to prior or ongoing chronic inflammation, can be accurately identified when combining features from steady state free precession as well as T2-weighted images with and without fat-suppression (Figure 7).

### Complications of CD

Complications of CD are also well shown in MRE and include: fistulas, phlegmons, abscesses and bowel obstruction. Fistulas and sinus tracts are demonstrated by the high signal intensity of their fluid content on steady-state free-precession and single-shot fast/turbo spin echo T2-weighted images, and enhancement of the linear tract on the post gadolinium T1-weighted sequences. Enter-enteric (Figure 8) and entero-colic fistulas are not uncommon. Fistulous communication with adjacent pelvic organs can also be seen. They should be suspected when crowded retracted and angulated small bowel loops are appreciated; known as star sign. Deep fissuring ulcers are occasionally appreciated, and better see on bSSFP images. Extra-enteric collections and abscesses (Figures 9 and 10) can be recognized by their fluid content and increased wall enhancement on post-gadolinium images. The ir-

regular morphology of an abscess cavity and appreciation of its rounded configuration on multiple planes allows distinction from tubular-shaped bowel.

Identifying active inflammation is rarely an interpretive problem in MRE. However, active inflammation can mask underlying fibrosis related to chronic disease of the bowel wall. In the setting of active inflammation, short-term MRE follow-up may be implemented to confirm improvements of active inflammation and to then evaluate the presence of unmasked chronic fibrotic disease<sup>[21]</sup>. It is important to identify fibrotic strictures because these are unresponsive to medical therapy and oftentimes require surgical intervention.

Assessment of inflammatory activity of CD is important to identify patients with active inflammation so that appropriate medical therapy may be prescribed. Given the advent of new medications some with serious side effects such as tumor necrosis factors alpha inhibitors, objective measures of activity are needed to justify their use and judge their effectiveness. Currently, there is no gold standard for determination of CD activity. Various authors have proposed MRE-based scoring systems for the assessment of inflammatory activity that includes features such as bowel wall thickening, lumen narrowing and the number of peri-intestinal lymph nodes<sup>[34-37]</sup>. However, these evaluation algorithms are relatively demanding, which may ultimately limit clinical utilization. Quantitative bowel enhancement parameters were found to correlate highly with histologic and endoscopic disease severity<sup>[30,38]</sup>. Although the perfusion analysis seems to be an accurate tool and correlates well with clinical parameters, it is relatively time consuming and requires special software and image post-processing. A recent study by Taylor *et al*<sup>[30]</sup> outlines another difficulty regarding perfusion analyses of the bowel wall. The use of DWI may also help in assessing disease severity and is thought to be a promising tool, especially if the use of a contrast agent is contraindicated<sup>[39]</sup>.

For clinical follow-up of patients with CD, MRE is the preferred examination of choice due to lack of ionizing radiation and allowance of more frequent monitoring, which is important given the costs and side effects asso-

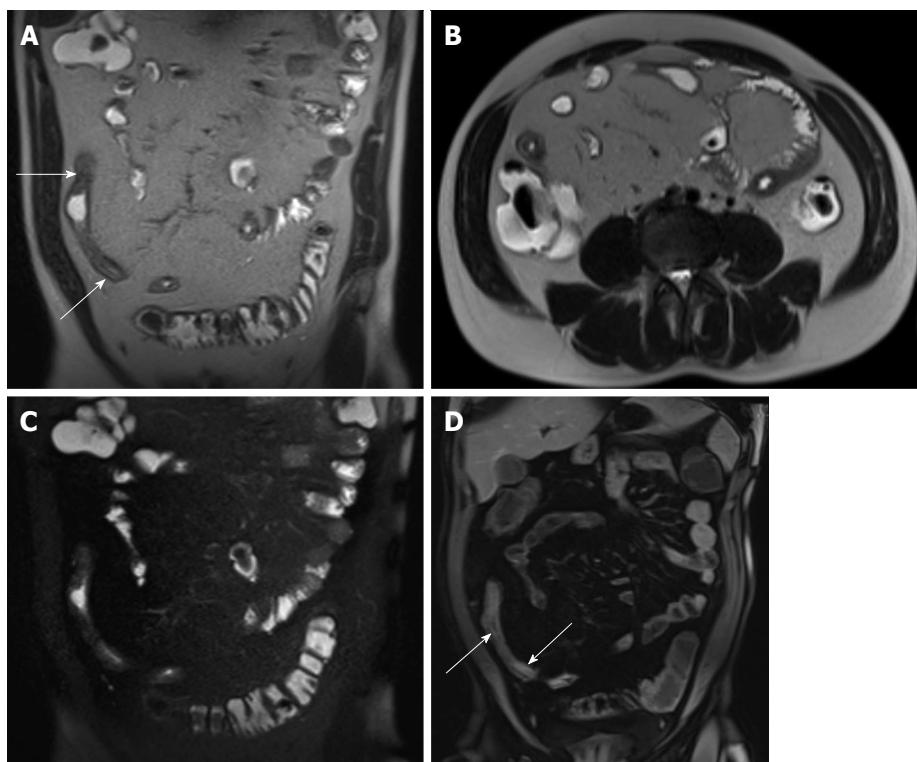


**Figure 7 Acute on chronic Crohn's disease.** A: Coronal and (B) axial T2-weighted single shot fast spin echo (SSFSE) as well as (C) coronal fat-suppressed T2-weighted SSFSE and (D) coronal fat-suppressed interstitial post-gadolinium 3D-GRE T1-weighted images during the interstitial phase. There is distal small bowel segment which demonstrates diffuse thickening and luminal narrowing (arrows, A), associated with submucosal high signal intensity on T2-weighted images (A and B) and with low-signal intensity on the fat-suppressed T2-weighted images (C), related to submucosal fat deposition, in keeping with chronic Crohn's disease. There is also a superimposed increased mucosal enhancement in affected bowel segments (arrows, D) and comb sign post-gadolinium images (D), reflecting disease activity, in keeping with acute on top of chronic disease. GRE: Gradient recalled echo.

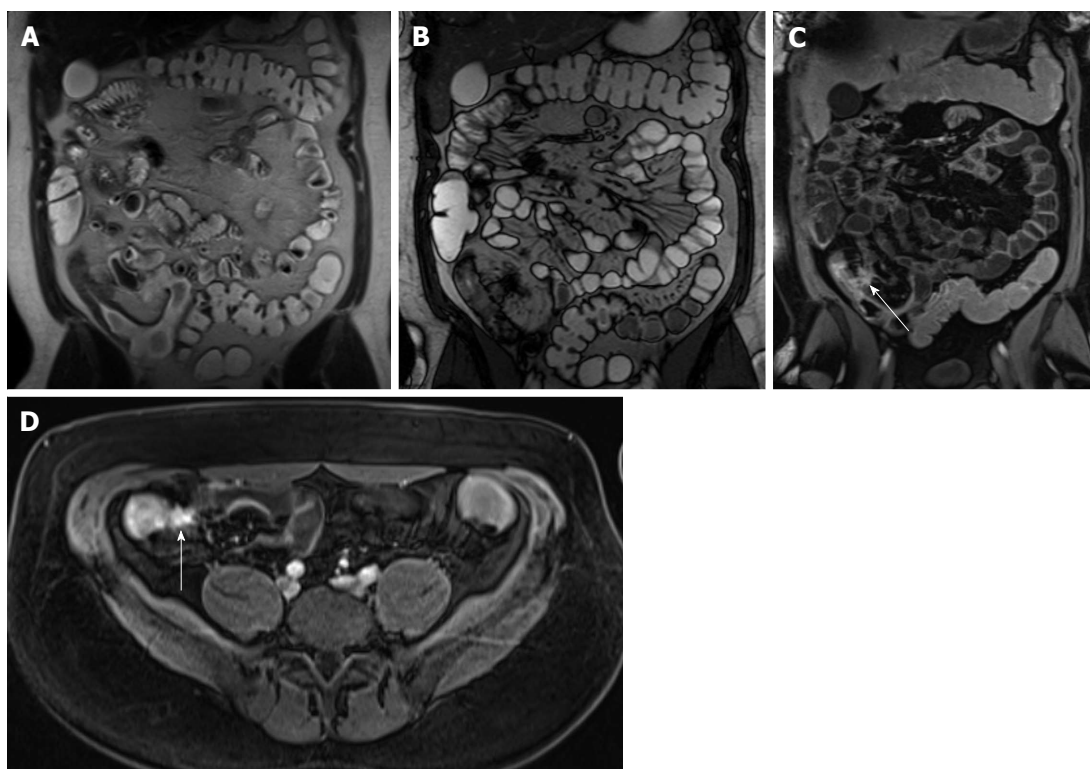


**Figure 8 Enteroenteric fistula in active Crohn's disease.** A: Coronal T2-weighted single shot fast spin echo and (B) coronal balanced steady state free precession images as well as (C) axial and (D) coronal fat-suppressed post-gadolinium 3D-GRE T1-weighted images during the (C) enteric and (D) interstitial phases. There is short-segment terminal ileal wall thickening (A and B), which shows extensive mucosal enhancement (C and D). There is also a linear tract extending from the involved segment to an adjacent ileal loop, showing increased enhancement, consistent with enteroenteric fistula (arrows, C and D). GRE: Gradient recalled echo.

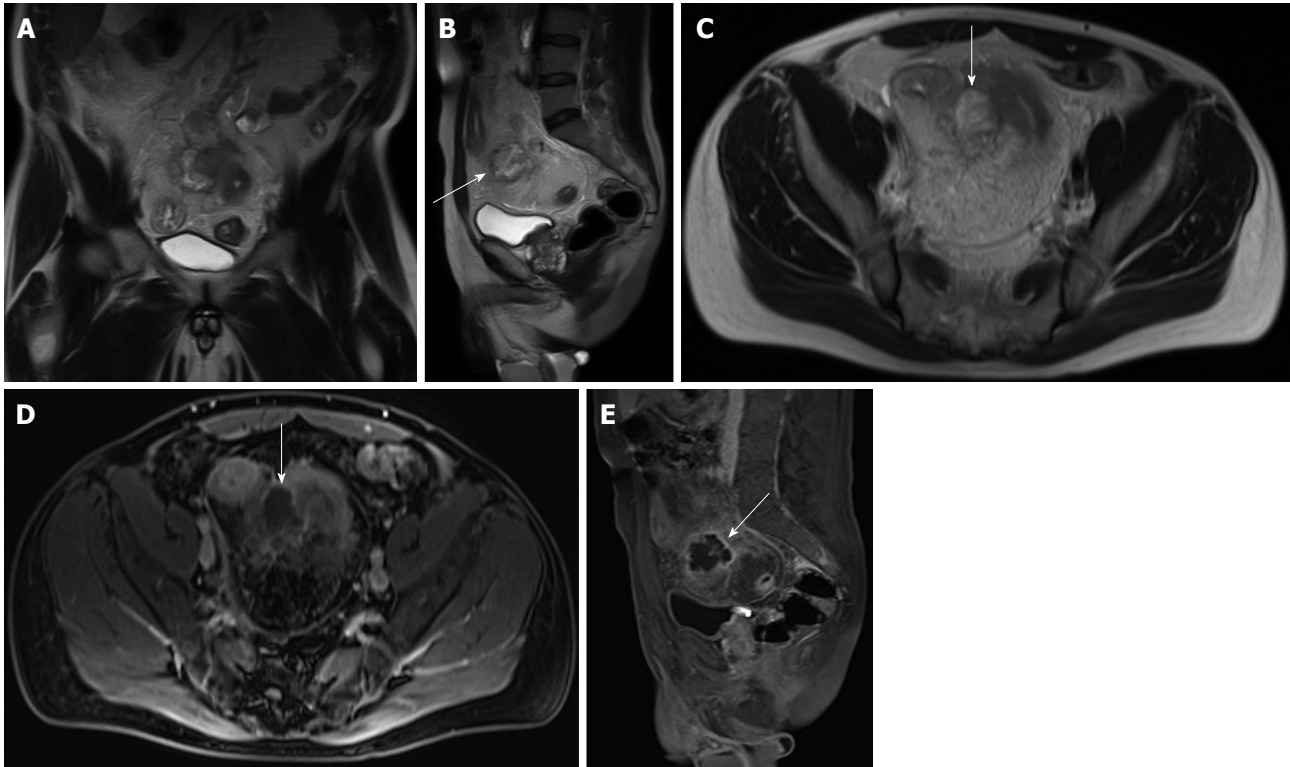


**Figure 9 Abscess formation complicating active Crohn's disease.** A: Coronal; B: Sagittal; C: Axial T2-weighted TSE images; D: Axial; E: Sagittal fat-suppressed post-gadolinium 3D-GRE T1-weighted images during the interstitial phase. Here is evidence of thickened small bowel loop segment and interloop mesenteric high T2 signal fluid collection (A, arrows, B and C) is noted, associated with rim enhancement (arrows, D and E) in keeping with mesenteric abscess formation complicating active Crohn's disease. GRE: Gradient recalled echo.

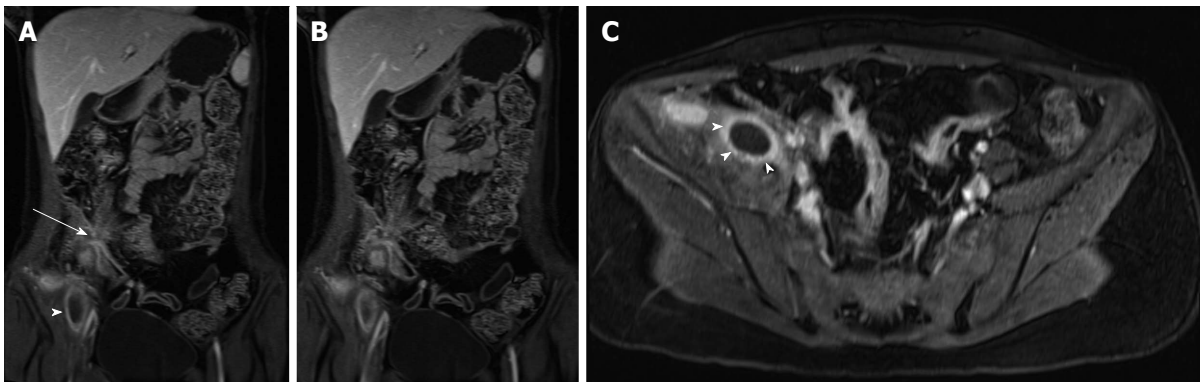


**Figure 10 Active distal ileal Crohn's disease with complex fistulization and iliopsoas abscess formation.** A and B: Coronal; C: Axial fat-suppressed post-gadolinium 3D-GRE T1-weighted images. There is evidence of terminal ileal thickening and enhancement in keeping with active Crohn's disease, associated with complex ileoileal and ileosigmoidal fistula formation (star sign, arrow, A and B) as well as iliopsoas inflammation and abscess formation (arrowheads, A, B and C). GRE: Gradient recalled echo.

ciated with medical treatment (Figure 11). Furthermore, MRE is also adequate for detection of recurrent disease following surgery (Figure 12).

## CELIAC DISEASE

Celiac disease is a permanent gluten-sensitive enteropathy of the gastrointestinal tract that affects the small intestine in genetically susceptible individuals. It is a systemic disease that may entail a variety of autoimmune disorders; the most important finding is an inflamed and flattened

small intestinal mucosa with impaired function<sup>[40]</sup>. The disease may present at any age and may show a wide range of clinical presentations of variable severity. The diagnosis of celiac disease can be challenging due to a wide range of clinical manifestations and the lack of specificity. Although the diagnosis is confirmed by small-intestine biopsy, patients who are referred for MRE with nonspecific gastro-intestinal complaints might have celiac disease as the underlying pathology.

MRE allow the visualization of the entire small bowel, and can demonstrate findings useful to suggest the

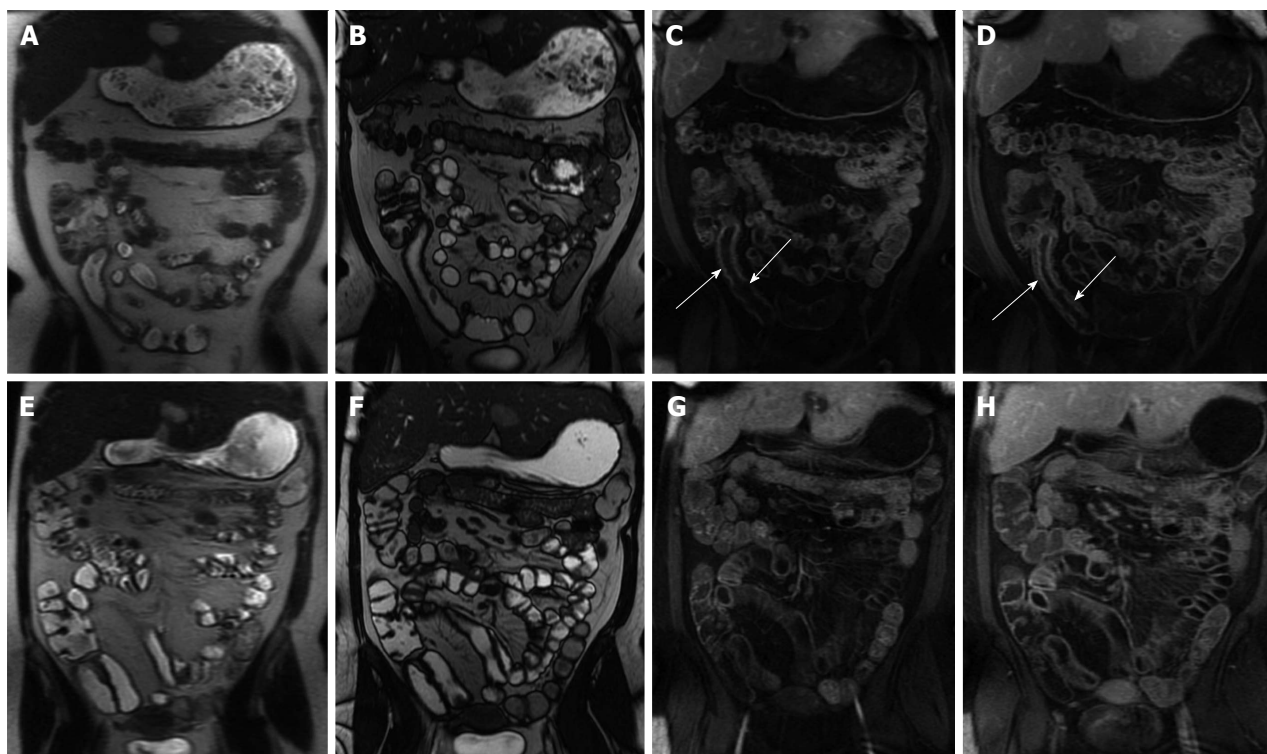


**Figure 11** Imaging followup in a patient with Crohn's disease. A and E: Coronal T2-weighted single shot fast spin echo; B and F: Coronal balanced steady state free precession images; C and G: Coronal; D and H: Axial fat-suppressed post-gadolinium 3D-GRE T1-weighted images. There is evidence of active Crohn's disease involving a long segment of the terminal ileum (A, B, C and D) in form of diffuse wall thickening and submucosal mucosal enhancement (arrows, C and D). Four-month re-evaluation shows interval decreased wall thickening and significant decreased mucosal/serosal enhancement, consistent with favourable response to medical therapy. GRE: Gradient recalled echo.

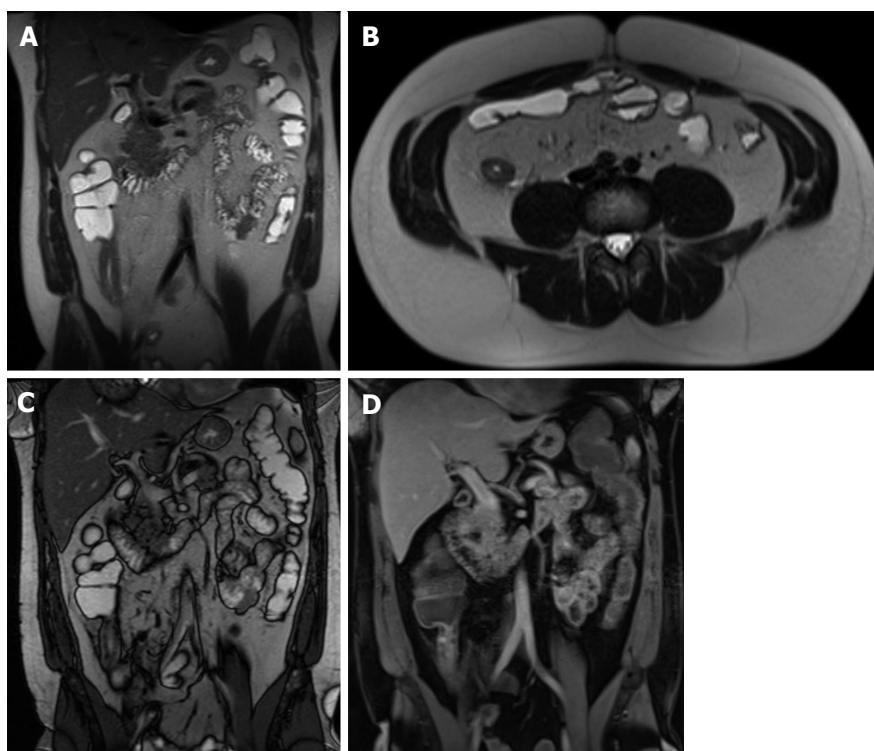


**Figure 12** Recurrent Crohn's disease post-surgery. A: Coronal; B: Axial T2-weighted single shot fast spin echo images; C: Coronal balanced steady state free precession; D: Coronal fat suppressed post-gadolinium 3D-GRE T1-weighted images. The patient is post distal ileal resection with a low-lying ileocolic anastomosis. The remaining distal ileum displays signs of active inflammation, namely bowel wall thickening and submucosal edema (A and B) associated with mucosal and serosal increased enhancement post-gadolinium (D) in keeping with recurrent Crohn's disease post-surgery. GRE: Gradient recalled echo.

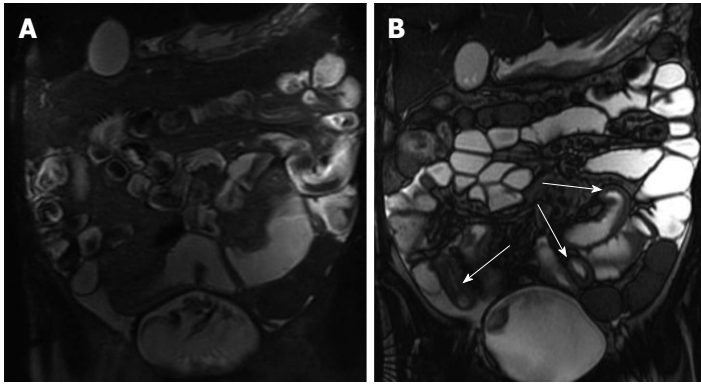


**Figure 13 Type 2 Gluten-sensitive enteropathy (Celiac disease).** A: Coronal T2-weighted single shot fast spin echo; B: Coronal balanced steady state free precession images show an abnormal ileal fold pattern with substantial decrease in the number of jejunal folds suggesting the diagnosis of celiac disease. Concomitantly, jejunal and ileal segments with increased mural thickening and stratification are seen (arrows, B), consistent with superimposed active inflammation.

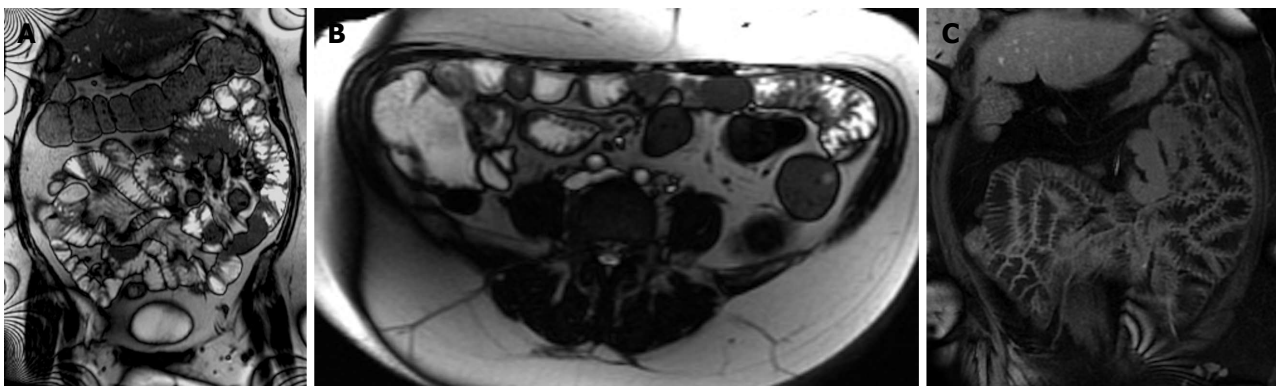


**Figure 14 Gluten-sensitive enteropathy (celiac disease).** A: Coronal T2-weighted single shot fast spin echo; B: Coronal balanced steady state free precession; C: Coronal fat-suppressed post-gadolinium 3D-GRE T1-weighted images during the interstitial phase. There is abnormal ileal fold pattern with increased number of folds mimicking the appearance of the jejunum (ileal jejunitization) in keeping with the diagnosis of celiac disease. GRE: Gradient recalled echo.

diagnosis of celiac disease in symptomatic adult patients. Among these findings, fold-pattern abnormality is the most distinctive<sup>[41,42]</sup>. Furthermore, because there are diseases that can resemble celiac disease histologically, MRE can help in excluding other disease entities<sup>[43]</sup>, such as lymphoma. Due to greater contrast resolution, MRE may be the preferred method of evaluation.

Fold-pattern abnormalities can best be assessed on bSSFP and single-shot fast/turbo spin-echo T2-weighted pulse sequences. A decreased number of jejunal folds (less than three folds per inch) or complete flattening of the folds can be seen in celiac disease (Figure 13). Also, the ileal folds can be increased (more than 5 folds per inch), a sign called “ileal jejunitization” (Figure 14). Jejunoileal fold pattern reversal is present when both ileal jejunitization and a decreased number of jejunal folds are present in the same patient. This fold-pattern reversal is very specific for celiac disease<sup>[41]</sup>. However, less specific imaging findings can be seen including strictures, lymphadenopathy, and perienteric stranding. Also, intussusception, visible as the “double halo sign” of bowel-within-bowel, and enlarged lymph nodes (> 1 cm)<sup>[41,42]</sup> are frequently encountered.

Small bowel lymphomas are associated with the concomitant presence of celiac disease<sup>[44]</sup> and should be suspected in cases in which considerable enlargement of

lymph nodes (> 2 cm) are identified.

## MISCELLANEOUS

Infectious diseases of the small bowel are the most prevalent disease processes in the small bowel after CD. *Yersinia enterocolitica* and *Campylobacter jejuni* represent the most common pathogens. Because of the increasing number of immunocompromised patients, the spectrum of pathogens has become wider during the past decades, including *Mycobacterium avium-intracellulare*, *Cryptosporidium* species, and cytomegalovirus. Infectious diseases may mimic CD; because they often manifest as terminal ileitis. Hence, clinical features always need to be considered in order to establish the correct diagnosis<sup>[45]</sup>.

The small bowel is highly sensitive to radiation exposure, with the ileum showing the lowest radiation tolerance. Radiation enteritis typically affects the distal ileum and is often associated with rectosigmoid involvement<sup>[46]</sup> (Figure 15). The rectum is affected more frequently than the small bowel in pelvic radiotherapy, where proctitis is estimated to occur in 19% of cases<sup>[47]</sup>. Typical imaging findings include luminal narrowing with small bowel obstruction and pre-stenotic dilatation as well as symmetric wall thickening and edema. Gadolinium-enhanced T1-

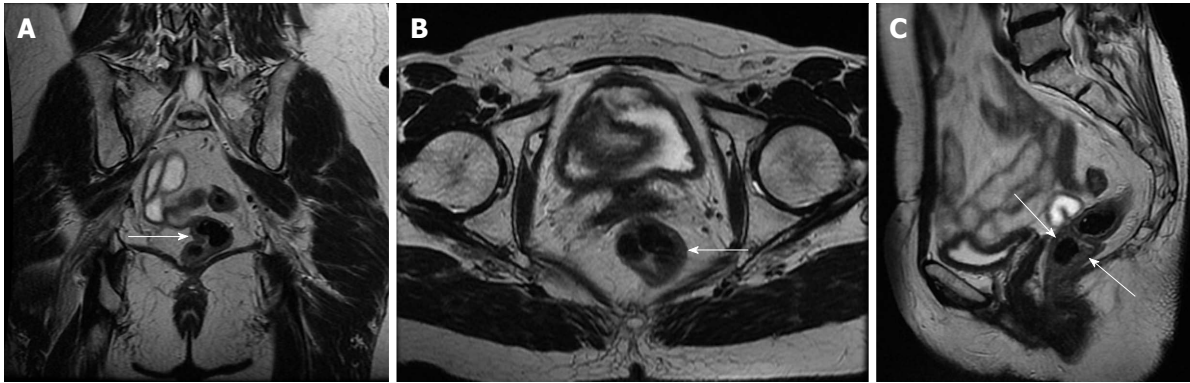


**Figure 15 Radiation proctocolitis.** A: Coronal; B: Axial; C: Sagittal T2-weighted TSE. The rectum and distal sigmoid colon demonstrates increased wall thickness with intermediate signal intensity on T2-weighted images (arrows, A, B and C). This patient underwent hysterectomy and radiation therapy. These findings are compatible with radiation proctocolitis. TSE: Turbo spin echo.

weighted images reveal increased enhancement in the affected bowel wall. Furthermore, submucosal edema can be depicted in early-stage radiation enteritis on T2-weighted images. Care is required to exclude malignancy, especially lymphoma, suggested by mass-like thickening, infiltration of adjacent tissues, and nodal enlargement<sup>[45]</sup>.

## PRACTICAL APPROACH TO INFLAMMATORY CONDITIONS-LARGE BOWEL

### Inflammatory bowel disease

CD and Ulcerative Colitis (UC) are the two main forms of chronic inflammatory bowel disease (IBD)<sup>[48]</sup> with 20%-25% of diagnoses being made during childhood<sup>[49]</sup>. Ileocolonoscopy with biopsy is the primary tool to make the diagnosis of colonic IBD. However, as mentioned above, intramural changes and extra-luminal abnormalities cannot be appreciated. Furthermore, concomitant small bowel involvement must be excluded.

Given the present role of MRE in small bowel CD, we believe that MRE  $\pm$  colonic enema (MR colonography) might have a similar role in colonic IBD. Often, the degree of distension of the large bowel achieved with oral contrast agents is suboptimal; however, previous reports have shown high sensitivity for differentiating type and severity of colonic IBD with comparable diagnostic accuracy to endoscopy<sup>[50]</sup>. Furthermore, a recent meta-analysis<sup>[51]</sup> suggested that MRI is a potentially effective method even without the administration of colonic enema. Recently, Rimola *et al.*<sup>[50]</sup> demonstrated that MRE in combination with a water-based enema is adequately able to assess disease activity in patients with established CD (Figure 16). Current evidence suggests adequate accuracy in evaluating disease activity in established IBD patients. Initial diagnosis and additional differentiation between UC and CD has not been defined yet. MRI findings of UC are similar to those of CD. UC is chronic inflammatory bowel disease restricted to the mucosa and distinctively limited to the colon (Figures 17 and 18) with a pre-

dictable distribution, *i.e.*, the disease begins in the rectum and extends proximally in a continuous fashion to involve part or the entire colon (pancolitis). In case of pancolitis, a backwash ileitis may also be present.

### Diverticulitis

MRI can effectively diagnose acute diverticulitis, with reported sensitivity of 86% to 94% and specificity of 88% to 92%<sup>[52]</sup>. It is likely that continually improving MRI techniques may result in higher sensitivity and specificity in the future. Buckley *et al.*<sup>[53]</sup> described MRI findings in patients with acute colonic diverticulitis, identifying findings similar to CT: bowel wall thickening, pericolic stranding, presence of diverticula (Figure 19), and presence of complications such as perforation and abscess formation<sup>[53]</sup>. MRI is also comparable to CT in its ability to identify alternative diagnoses<sup>[54]</sup>.

### Appendicitis

Traditionally, acute appendicitis has been diagnosed on the basis of clinical findings. Despite having high sensitivity (up to 100%), clinical evaluation has relatively low specificity (73%)<sup>[55]</sup>. The exact role of imaging in the setting of suspected appendicitis is still a matter of debate. CT is the preferred imaging technique for the diagnosis and assessment of appendicitis in the United States<sup>[56]</sup> and has been shown to reduce the negative-finding appendectomy rate from 24% to 3%<sup>[57]</sup>. There are several individual CT findings that suggest a diagnosis of appendicitis like appendiceal enlargement (> 6 mm in diameter) that has a high positive predictive value<sup>[58]</sup>. Likewise, the sensitivity of adjacent fat infiltration is high for the diagnosis of appendicitis<sup>[59]</sup>. However, the visualization of an appendicolith has been shown to have a low positive predictive value for the diagnosis of appendicitis<sup>[58]</sup>. Complications, such as perforated appendicitis, extraluminal gas or abscess can be diagnosed with high specificity<sup>[60]</sup>. If appendicitis can be ruled out, the most common alternative imaging-based diagnoses are gynecologic diseases, diverticulitis, colitis, or epiploic appendagitis<sup>[61]</sup>.

MRI has demonstrated promising accuracy for the

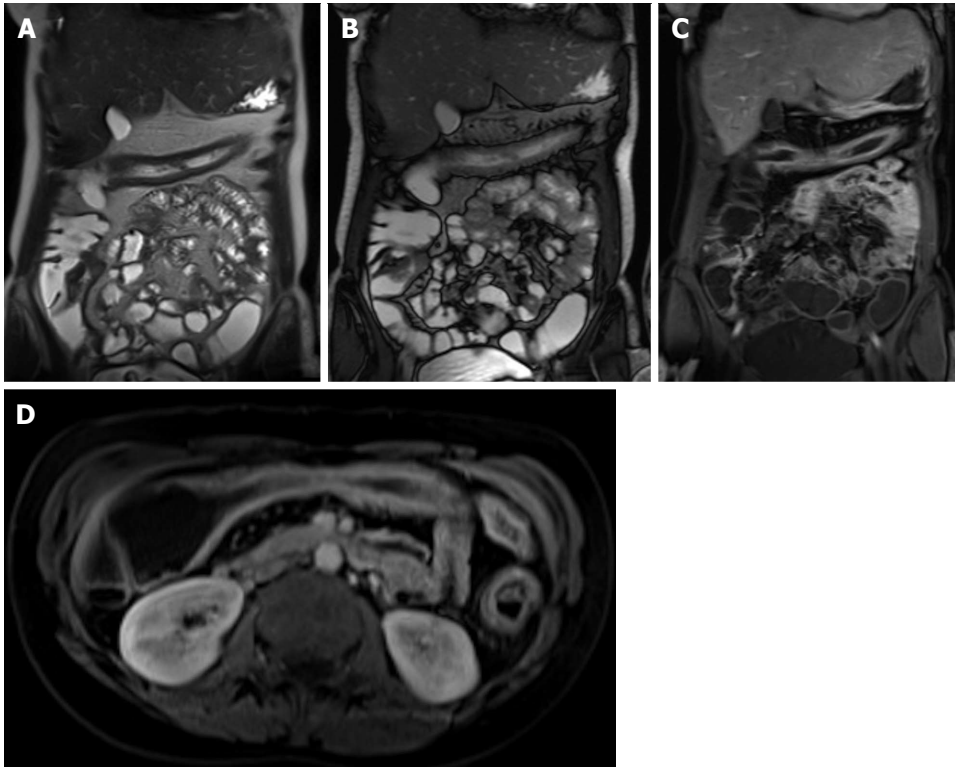


**Figure 16 Crohn's colitis.** A: Coronal T2-weighted single shot fast spin echo; B: Coronal balanced steady state free precession images; C: Coronal; D: Axial fat-suppressed post-gadolinium 3D-GRE T1-weighted images. There is a segmental uniform thickening of the transverse colon associated with submucosal edema (A and B), mucosal hyper-enhancement, and engorgement of the supplying mesenteric vessels (C and D) in keeping with active Crohn's colitis. Also of note is the focal hyper-enhancement of the terminal ileum (C). GRE: Gradient recalled echo.

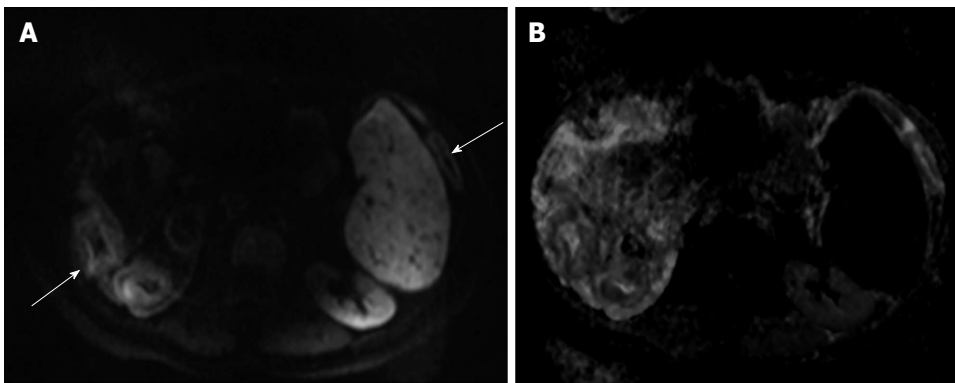


**Figure 17 Active colonic ulcerative colitis.** A: Axial diffusion-weighted imaging ( $b = 650 \text{ s/mm}^2$ ); B: ADC map images. There is diffuse thickening involving the colon associated with diffuse mucosal diffusion restriction (arrows A) in keeping with active ulcerative colitis. ADC: Analog-digital conversion.

assessment and diagnosis of appendicitis, albeit in a relatively small series of patients, who often were pregnant (Figure 20)<sup>[62]</sup>. A recent study showed that the accuracy of conditional or immediate MRI was similar to that of conditional CT in patients suspected of having appendicitis<sup>[63]</sup>. However, due to the non-wide availability of MRI systems, relative lack of required expertise and extensive cost-effectiveness studies; the role of MRI is somewhat limited. At this time, MRI is used in only select cases at many institutions, primarily after ultrasound yields nondiagnostic findings in pregnant women.

As in CT, the inflamed appendix and surrounding tissues show marked enhancement on gadolinium-enhanced

T1-weighted fat-suppressed images. Recently, Leeuwenburgh *et al.*<sup>[64]</sup> suggested that the most significant MRI features of acute appendicitis include appendix enlargement (diameter > 7 mm), peri-appendiceal fat stranding, and restricted diffusion of appendiceal wall; the presence of all these three features on MRI leads to a correct diagnosis of 96%, whereas their absence practically rules out appendicitis.

## GASTRIC AND SMALL BOWEL TUMORS

### Gastric tumors

**Adenocarcinoma:** Gastric carcinoma is one of the most

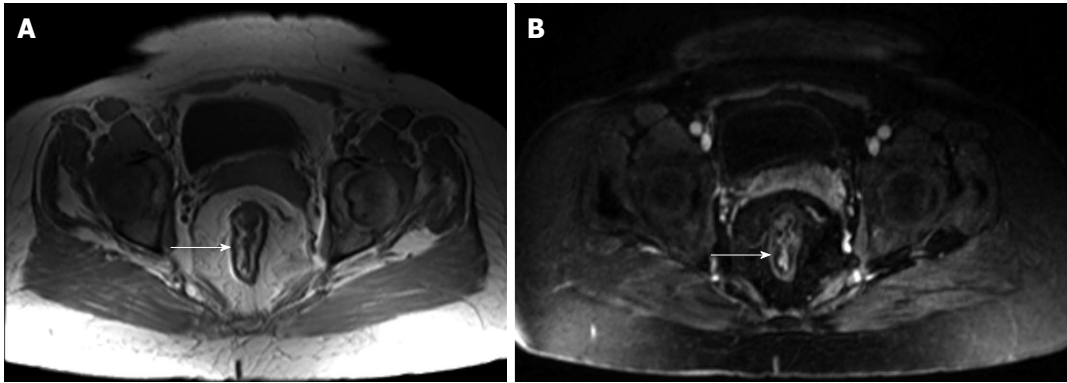


**Figure 18 Chronic ulcerative colitis.** A: Axial in-phase T1-weighted; B: Axial fat-suppressed post-gadolinium 3D-GRE T1-weighted images. There is diffuse rectal submucosal increased T1 signal (arrow, A), which demonstrates low signal on fat-suppression (arrow, B), but no significant arterial enhancement (B), in keeping with chronic ulcerative colitis. GRE: Gradient recalled echo.

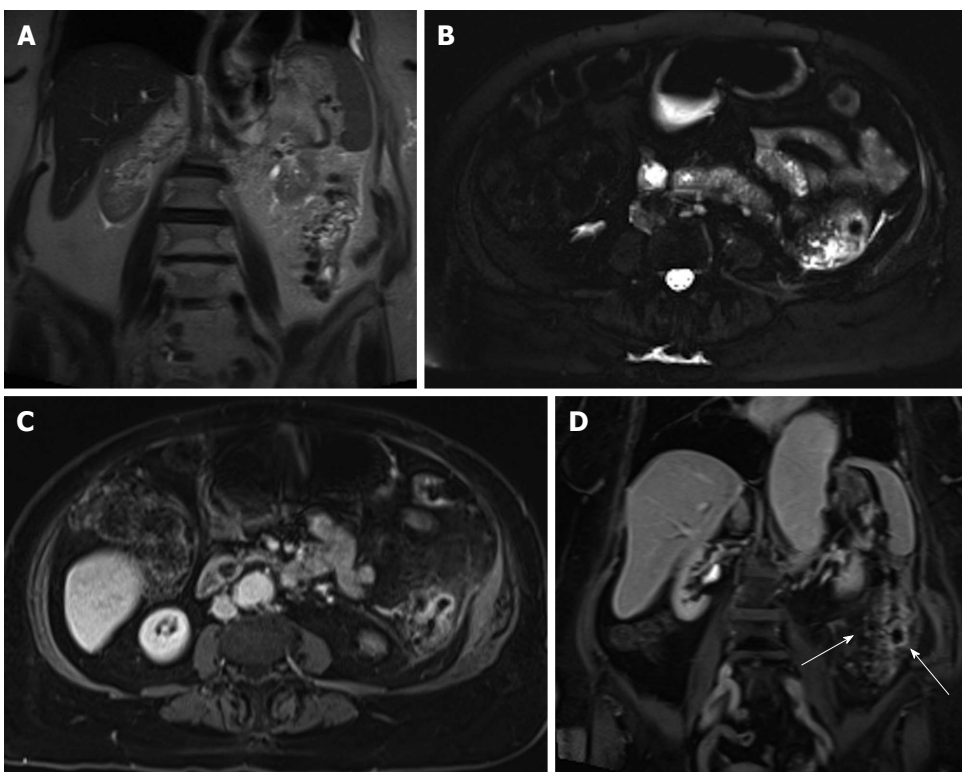


**Figure 19 Left colonic diverticulitis.** A: Coronal T2-weighted single shot fast spin echo (SSFSE); B: Axial fat-suppressed T2-weighted SSFSE; C: Axial and D: Coronal fat-suppressed post-gadolinium 3D-GRE T1-weighted images during the interstitial phase. There is wall thickening of the descending colon (A), with pericolic free fluid, better depicted on axial T2-weighted SSFSE image (B). Post-gadolinium images (C and D) show marked enhancement of the left colon, with pericolic enhancement including the pre-renal fascia. Coronal postgadolinium image (D) shows left colonic diverticula and associated bowel wall and vasa recti engorgement (arrows), consistent with inflammation. GRE: Gradient recalled echo.

common causes of cancer-related death worldwide. Borrmann proposed the original classification of advanced gastric cancer in 1926 based on macroscopic evaluation of the tumor. Advanced gastric cancer was classified by Borrmann as fungating (type 1), excavated (type 2), ulcerated infiltrating (type 3), and diffusely infiltrating (type 4) based on shape and infiltration margin. The prognosis of this disease depends on a variety of factors including Borrmann classification<sup>[65]</sup>.

It is generally accepted that the goals of MRI is to demonstrate the primary tumor, but also assess the

depth of invasion and detect extra gastric disease<sup>[66,67]</sup>. On gadolinium-enhanced fat-suppressed T1-weighted images, the tumor shows heterogeneous enhancement compared to normal gastric wall. Infiltrative tumors (linitis plastica) enhances modestly (Figure 21). In contradistinction, other morphologic types enhance more intensely; however, these tend yet to be better demonstrated in the arterial phase, as normal gastric mucosa tends to enhance substantially. Previous studies have shown that MRI has similar diagnostic accuracy in the diagnosis and preoperative staging of gastric cancer compared to

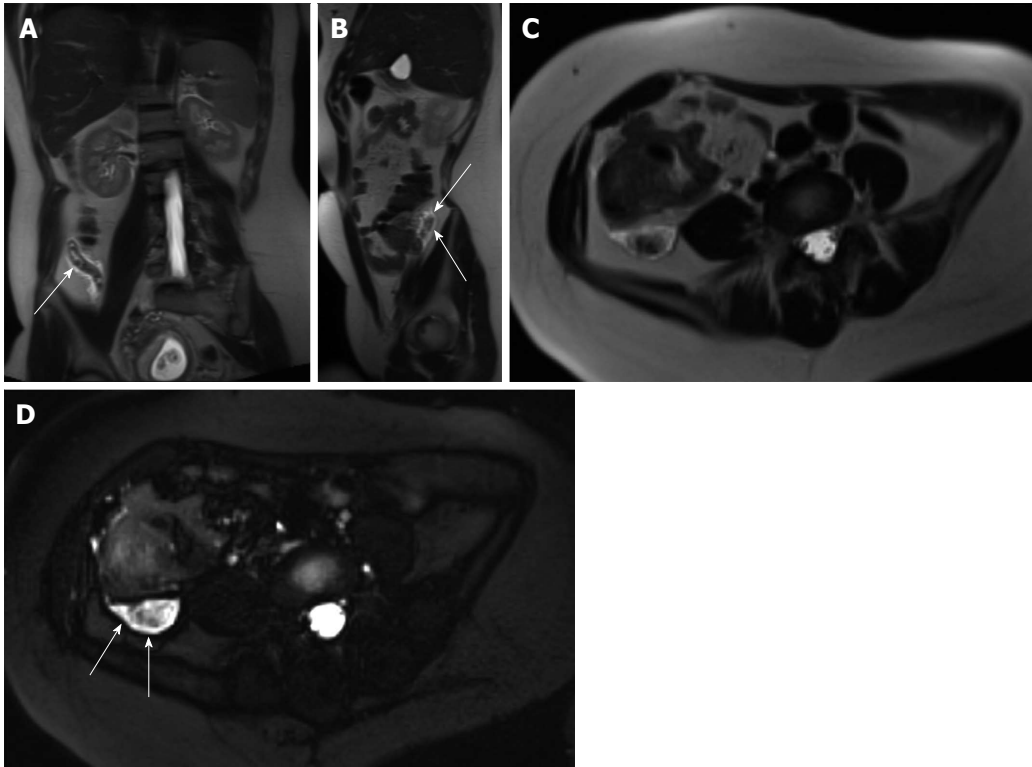


**Figure 20 Acute appendicitis in a pregnant patient.** A: Coronal; B: Sagittal; and C: Axial single shot fast spin echo (SSFSE) T2 as well as D: fat-suppressed SSFSE T2 images. There is a blind-ended tubular structure at the retrocecal region (arrows, A, B) associated with uniform, diffuse wall thickening and dilatation, reaching up to 13 mm in diameter (C and D) as well as periappendiceal edema and small periappendiceal fluid (A-D) collection, in keeping with acute appendicitis. Edema and fluid appear significantly more conspicuous on fat-suppressed images (arrows, D). Noted is a gravid uterus (A).

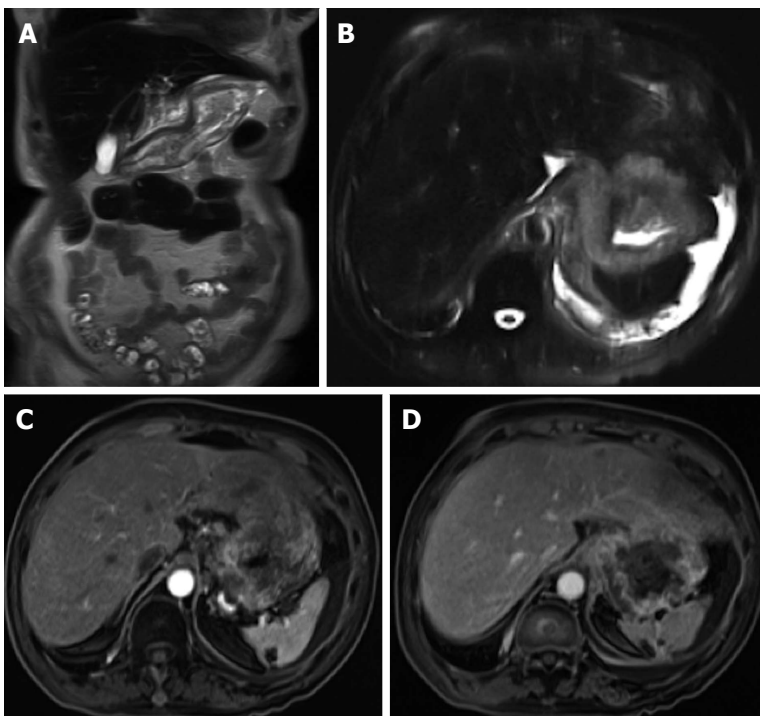


**Figure 21 Gastric adenocarcinoma.** A: Coronal T2-weighted single shot fast spin echo (SSFSE); B: Axial fat suppressed T2-weighted SSFSE; C: Axial arterial; D: Interstitial post-gadolinium 3D-GRE T1-weighted images. There is diffuse heterogeneous wall thickening of the stomach (A and B) with heterogeneous enhancement (C and D) consistent with linitis plastica. GRE: Gradient recalled echo.

multidetector CT<sup>[67]</sup>. Maccioni *et al*<sup>[67]</sup> have shown similar detection rate of gastric lesions; however, the T staging

accuracy for gastric cancer was superior for MRI (60% *vs* 48%). This aspect has been previously described by Sohn

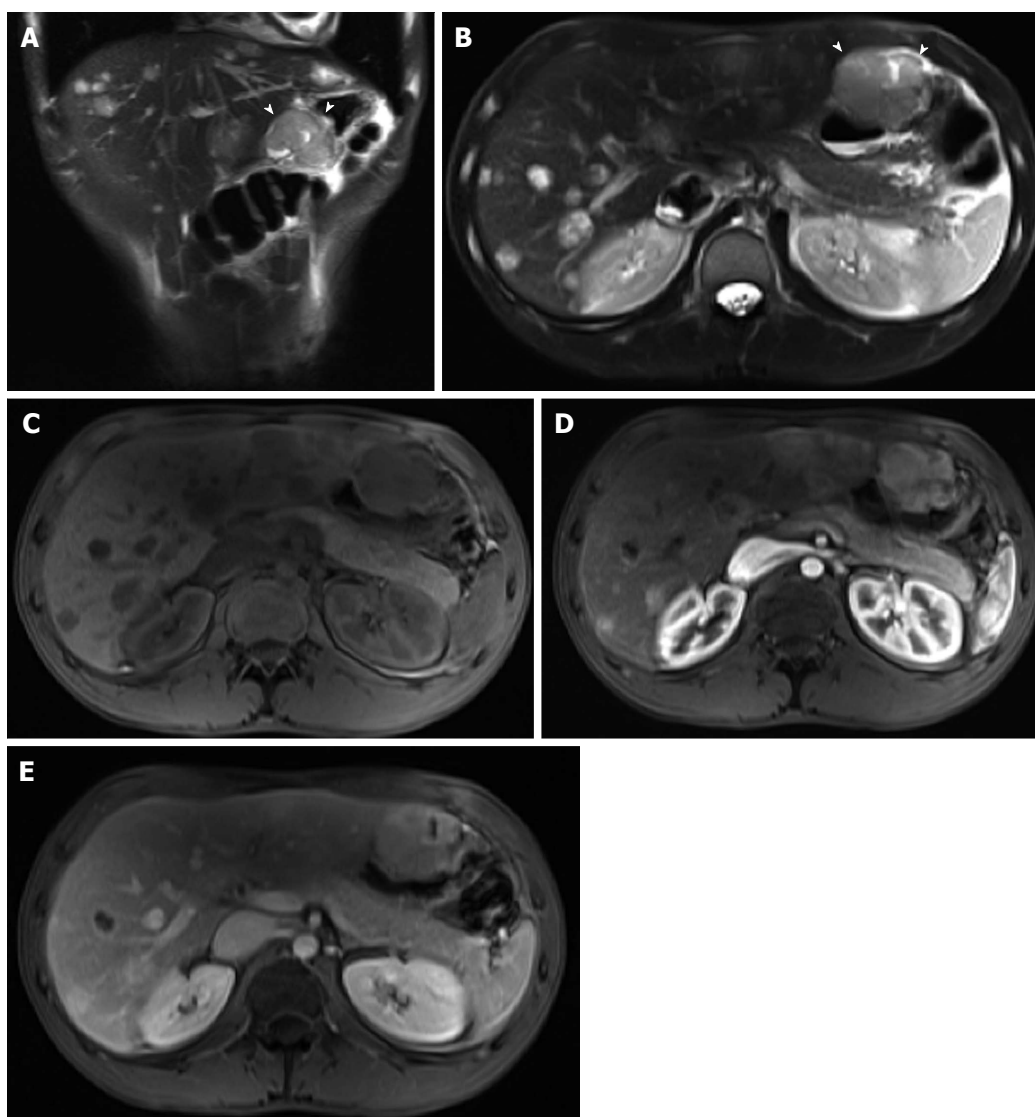


**Figure 22 Metastatic malignant gastric gastrointestinal stromal tumors.** A: Coronal T2-weighted single shot fast spin echo (SSFSE); B: Axial fat suppressed T2-weighted SSFSE; C: Pre- and post-gadolinium 3D-GRE T1-weighted images during the (D) arterial and (E) interstitial phases. There is a hyperintense mass within the wall of the gastric antrum, which abuts the edge of the left lobe of the liver; Central necrosis is seen (arrowheads, A and B). Multiple liver lesions show heterogeneously increased T2 signal and hypervascular characteristics, fading to isointensity on late phase of enhancement, consistent with metastases. GRE: Gradient recalled echo.

*et al*<sup>[68]</sup> showing a slightly improved accuracy with MRI (73.3% *vs* 66.7%). The presence of involved lymph nodes is acknowledged to be an independent factor of poor prognosis. The overall accuracy for nodal staging with MRI is similar to that attained with CT<sup>[67,68]</sup>.

**Gastrointestinal stromal tumors:** Gastrointestinal stromal tumors (GISTs) are the most common mesenchymal neoplasms, which can occur anywhere in the GI tract. Approximately 60%-70% of GISTs occur in the stomach, followed by the small intestine at 25%-35%<sup>[69]</sup>. GISTs can either grow into the mucosa causing ulceration or protrude towards the serosal side<sup>[70]</sup>. These are solid tumors that can undergo liquefactive necrosis and intratumoral hemorrhage. On MRI, the tumor's large size coupled with intense enhancement and regions of necrosis are typical features of GISTs. Moreover, MRI may be helpful in determining the organ of origin in large tumors, as

well as detecting metastases of GISTs involving the liver and peritoneum (Figure 22). Also, MRI can provide additional information on the tumor response to medical treatment<sup>[71]</sup>.

**Lymphoma:** The stomach is the most commonly involved site in GI tract, followed by the small bowel (ileo-cecal region) and rectum<sup>[72]</sup>. Diffuse gastric wall thickening is almost always present in gastric lymphoma (Figure 23). Lymphoma also has other characteristics including homogeneous T2 signal intensity, substantial lymph nodes enlargement, and splenomegaly<sup>[73]</sup>.

#### **Small bowel tumors**

The incidence of primary tumors is low, accounting for approximately 1% to 3% of all gastrointestinal tumors. Although small bowel tumors are rare, they are commonly considered in the differential diagnosis of small

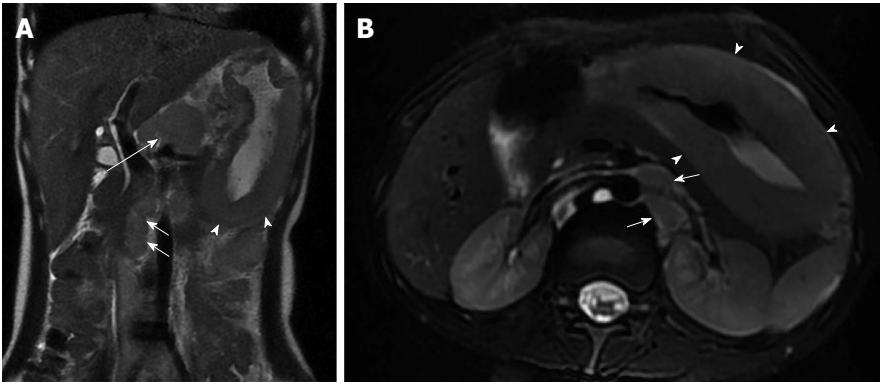


**Figure 23 Non-Hodgkin lymphoma of the stomach.** A: Coronal T2-weighted single shot fast spin echo (SSFSE) and (B) axial fat-suppressed T2-weighted SSFSE images. There is marked, diffuse, asymmetric gastric wall thickening with smooth outlines, predominantly involving the gastric body and antrum, associated with mildly increased heterogeneous T2 signal intensity (arrowheads, A and B), large conglomerate nodal mass at the gastrohepatic ligament (long arrow, A), and multiple enlarged retroperitoneal lymph nodes (short arrows A and B). Constellation of findings is diagnostic of non-Hodgkin gastric lymphoma with diffuse abdominal lymphadenopathy.

bowel disease because of their nonspecific presenting symptoms such as pain, obstruction, bleeding, and weight loss.

Secondary intestinal tumors, which originate from other parts of the body and metastasize to the small intestine, are clinically common and may cause symptoms similar to primary intestinal neoplasms<sup>[74]</sup>. MRE has been shown to be a useful technique for the study of suspected bowel masses<sup>[75]</sup>. Factors that affect the diagnostic performance of a specific modality include the size and characteristics of the tumor, extra-enteric extension, and eventual small bowel obstruction. The degree of distention and motion artifacts also influences the quality of the study. Although there is paucity of data regarding the sensitivity of MRE for the detection of small-bowel masses, one study showed no significant difference between MRI and wireless capsule endoscopy for the detection of large, clinically significant polyps in patients with polyposis syndromes with additional advantage of improved localization with MRE<sup>[11]</sup>.

On MRE, hyper-enhancing masses are usually well depicted when biphasic enteric contrast material is administered. Although any tumor may appear as focal intraluminal mass, location along the GI tract (duodenal, jejunal, or ileal), as well as focal areas of bowel wall thickening or areas of increased mural enhancement, suggest the presence of a tumoral mass. For example, a pedunculated or predominantly exophytic mass suggests a gastrointestinal stromal tumor<sup>[76]</sup> (Figure 24), while an exophytic mass combined with adjacent lymphadenopathy with or without significant dilatation of the small bowel suggests small bowel lymphoma<sup>[76]</sup> (Figure 25). Carcinoid tumors arise from neuroendocrine precursors or small bowel wall and may manifest as hypervascular masses, often in the ileum or as enhancing carpet lesions, mimicking the wall thickening of CD. Mesenteric carcinoid metastases demonstrate a desmoplastic reaction that may contain eccentric calcifications (not depicted on MRE) or may be clustered near the mesenteric root<sup>[77]</sup> (Figure 26). Carcinoid metastases to the liver can appear hypervascular and usually show washout on the delayed imaging mimicking

hepatocellular carcinomas (Figure 26). Adenocarcinomas assume a variety of shapes but are generally located in the proximal small bowel (Figure 27) and typically result in proximal dilatation greater than that observed with other neoplasms.

## COLORECTAL TUMORS

### Colorectal adenocarcinoma

Ninety-six percent of colorectal cancers are adenocarcinomas<sup>[78]</sup>. A combination of thin-section 3D-GRE fat-suppressed gadolinium-enhanced T1-weighted and high-resolution T2-weighted fast-spin echo (FSE) provides excellent information about tumor size, bowel wall involvement, peri-tumoral extension, and lymph node detection; especially for tumors located proximally to rectal ampulla<sup>[79,80]</sup>.

MRI has established itself as the primary method for local staging as well as preoperative planning and post-neoadjuvant assessment of the rectal cancers. Rectal cancer MRI evaluation requires a dedicated protocol. The only sequence that is required is a high-resolution T2-weighted fast spin echo. Sagittal plane images are initially acquired, followed by axial and coronal images perpendicular to the rectal wall at the level of the tumor, termed short- and long-axis images, respectively. With high-resolution T2-weighted imaging as a gold standard sequence, it proved to be superior in T staging, especially when the patient's comfort and acceptance are taken into consideration<sup>[81-83]</sup>. The ability of MR to delineate the mesorectal fascia and related structures makes it effective to accurately predict curative resection of the rectal cancer<sup>[81,84]</sup>.

Practical aspects of rectal cancer MR staging include tumor size evaluation, longitudinal and axial localization, tumor extent through the rectal wall layers, extramural invasion of the mesorectal fat and/or mesorectal fascia as well as deep pelvic organs invasion or anal canal extension in case of low lying rectal tumors. Short-axis T2 high-resolution imaging is critical for more accurate tumor (T) staging and yields higher accuracy for deeper tumoral extension (T3-4) (Figure 28); however, transrec-

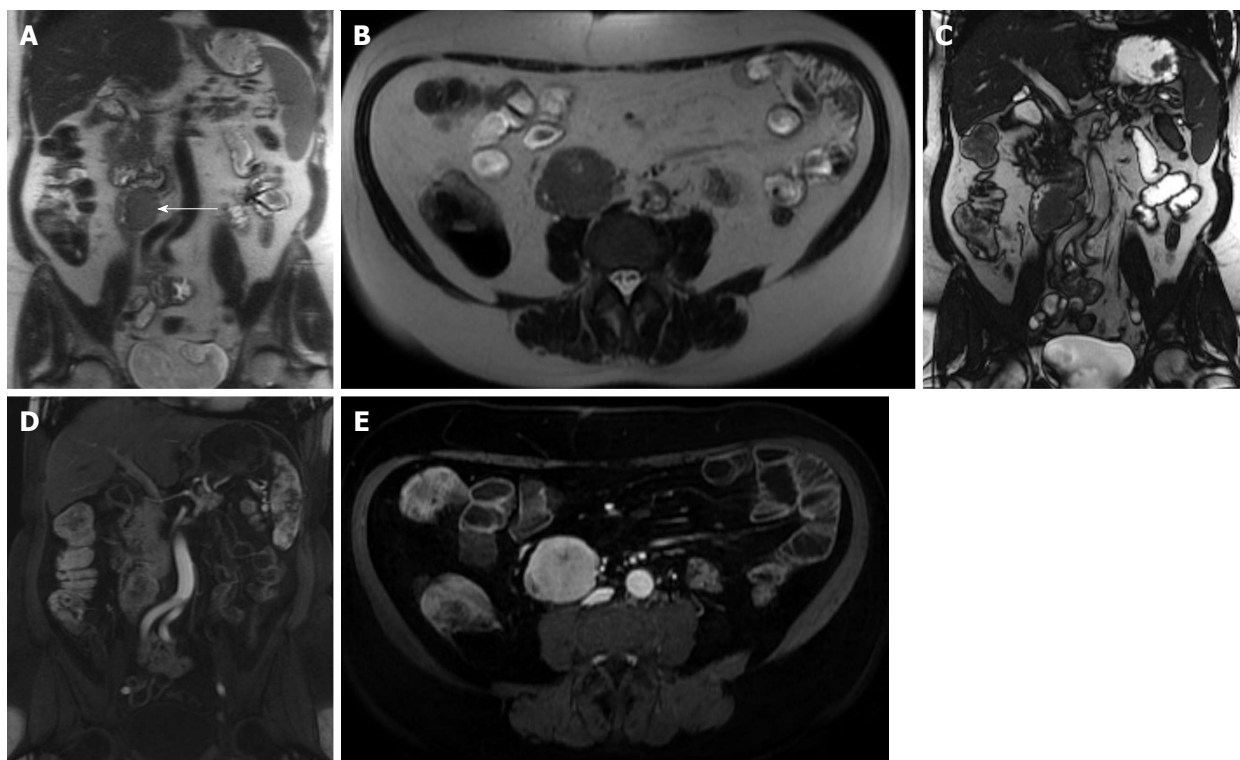


**Figure 24 Jejunal gastrointestinal stromal tumor.** A: Coronal and (B) axial T2-weighted single shot fast spin echo, and (C) coronal balanced steady state free precession images as well as (D) coronal and (E) axial fat-suppressed post-gadolinium 3D-GRE T1-weighted images. There is a well-defined intramural, exophytic mass lesion arising from the proximal jejunum, in a patient with malrotation, which demonstrates intermediately increased T2 signal (arrow, A, B), early moderate hypervascularity (D) and progressive enhancement (E) post-gadolinium associated with a tiny central area of necrosis in keeping with jejunal gastrointestinal stromal tumor. Lack of proximal bowel obstruction is consistent with its eccentric origin. GRE: Gradient recalled echo.

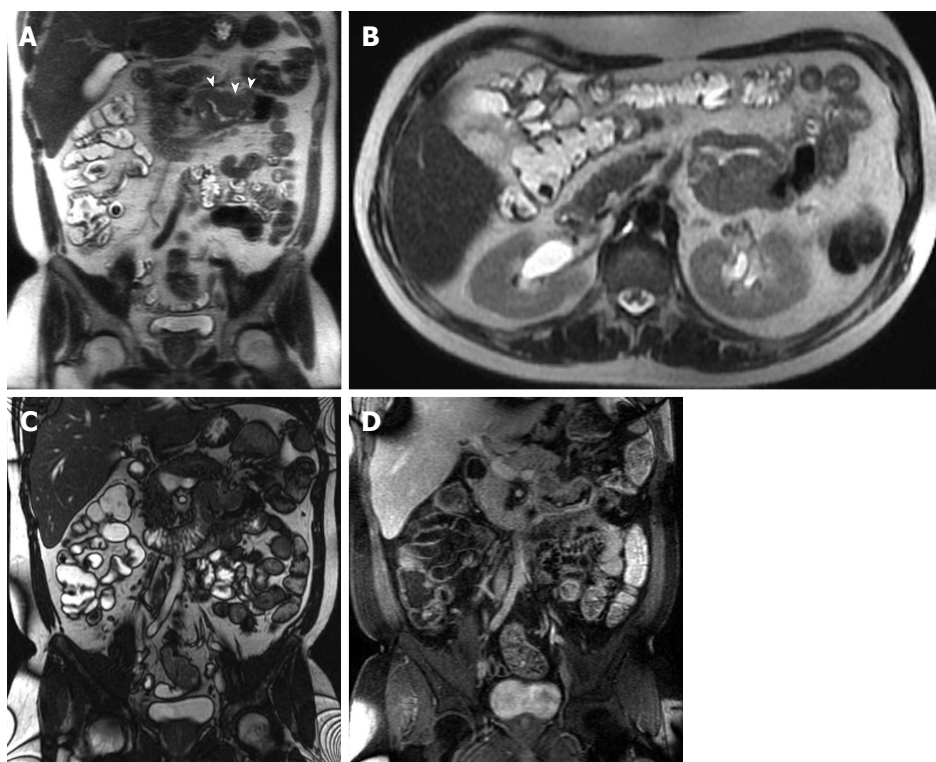


**Figure 25 Jejunal lymphoma.** A: Coronal and (B) axial T2-weighted single shot fast spin echo, (C) coronal balanced steady state free precession, and (D) coronal fat-suppressed post-gadolinium 3D-GRE T1-weighted images. There is a short segment of proximal jejunal circumferential, irregular, asymmetric wall thickening resulting in luminal narrowing (arrowheads, A) and demonstrates intermediate T2 signal (A and B) and mild enhancement post-gadolinium (D) in keeping with a pathologically proven jejunal lymphoma. GRE: Gradient recalled echo.

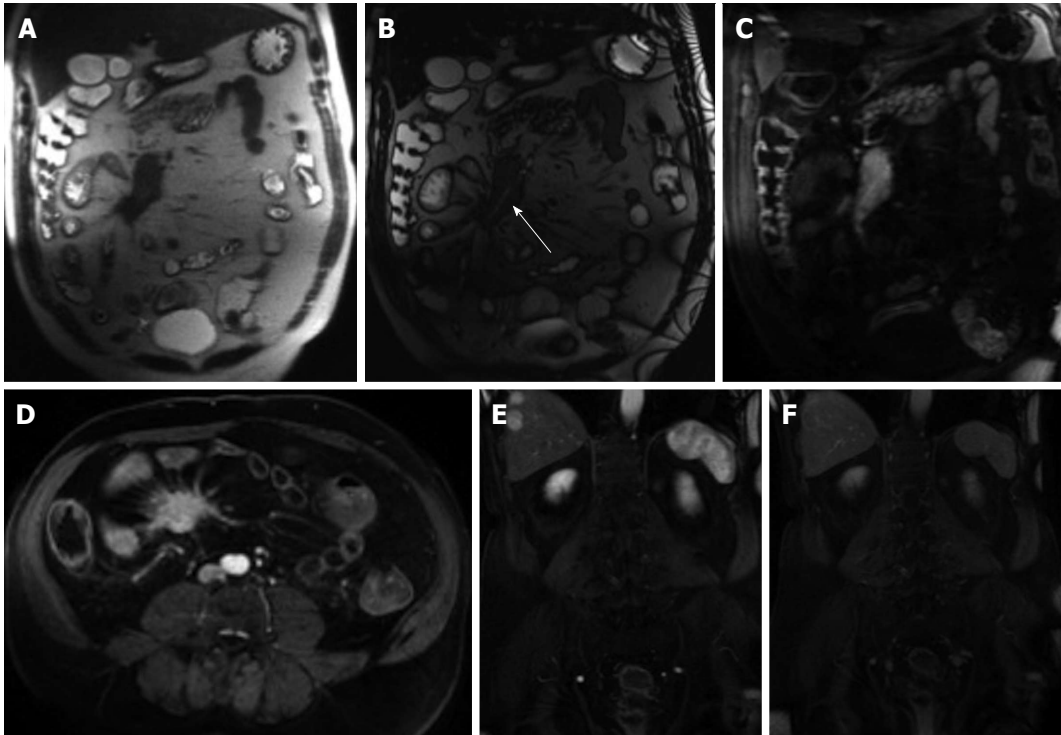


**Figure 26 Mesenteric carcinoid.** A: Coronal T2-weighted single shot fast spin echo; B: Coronal balanced steady state free precession; C and D: Coronal arterial; E: Axial enteric; F: Coronal interstitial fat-suppressed post-gadolinium 3D-GRE T1-weighted images. There is a large mesenteric mass encasing the superior mesenteric artery and its branches (arrow, B) associated with desmoplastic reaction and small bowel retraction noted on pre-contrast images (A, B), which demonstrates hypervascular (C) and typical sunburst margins (D). Liver metastases are seen with the typical wash-in (D) and washout (F) appearance mimicking the appearance of hepatocellular carcinoma. GRE: Gradient recalled echo.

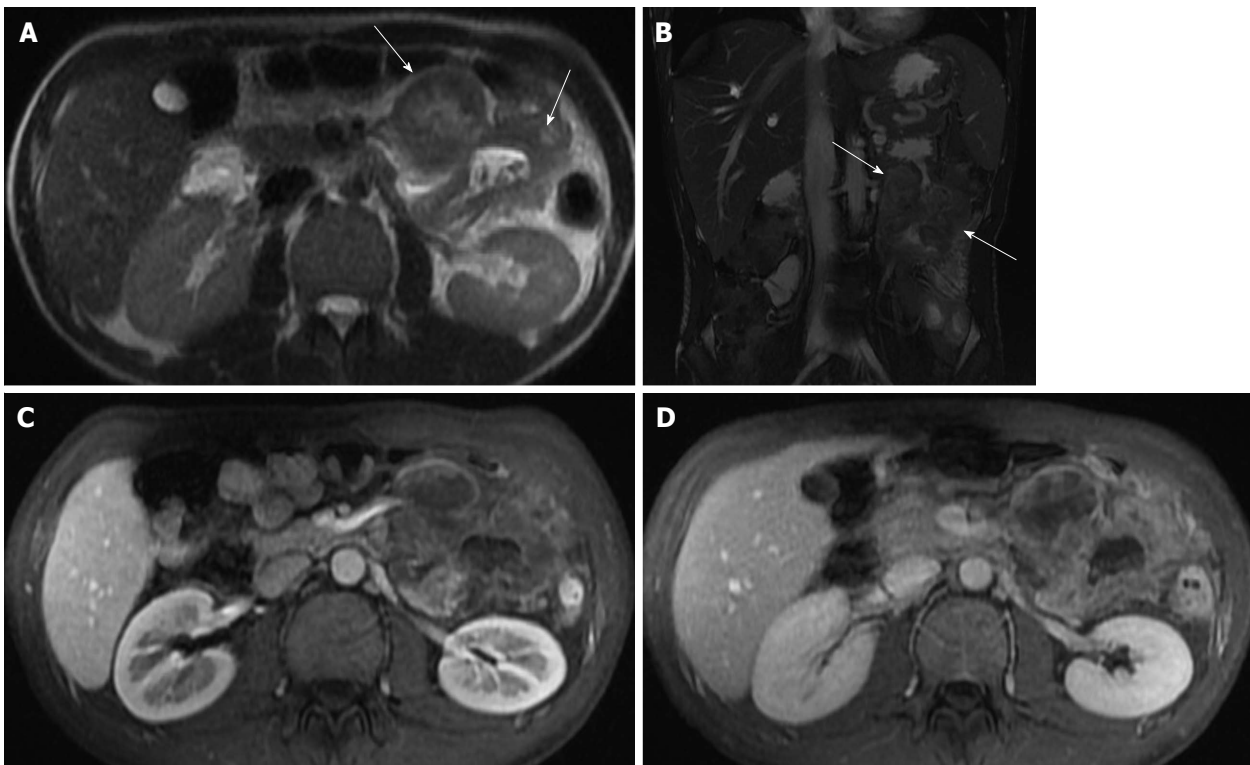


**Figure 27 Jejunal adenocarcinoma.** A: Axial T2-weighted single shot fast spin echo and (B) coronal balanced steady state free precession images as well as axial fat-suppressed post-gadolinium 3D-GRE T1-weighted images during the (C) hepatic arterial dominant and (D) hepatic venous phases. There is significant circumferential, irregular, asymmetric wall thickening of the proximal jejunum with exophytic extension (arrows, A and B) and hypovascular enhancement pattern (C and D) in keeping with a pathologically proven jejunal adenocarcinoma. GRE: Gradient recalled echo.

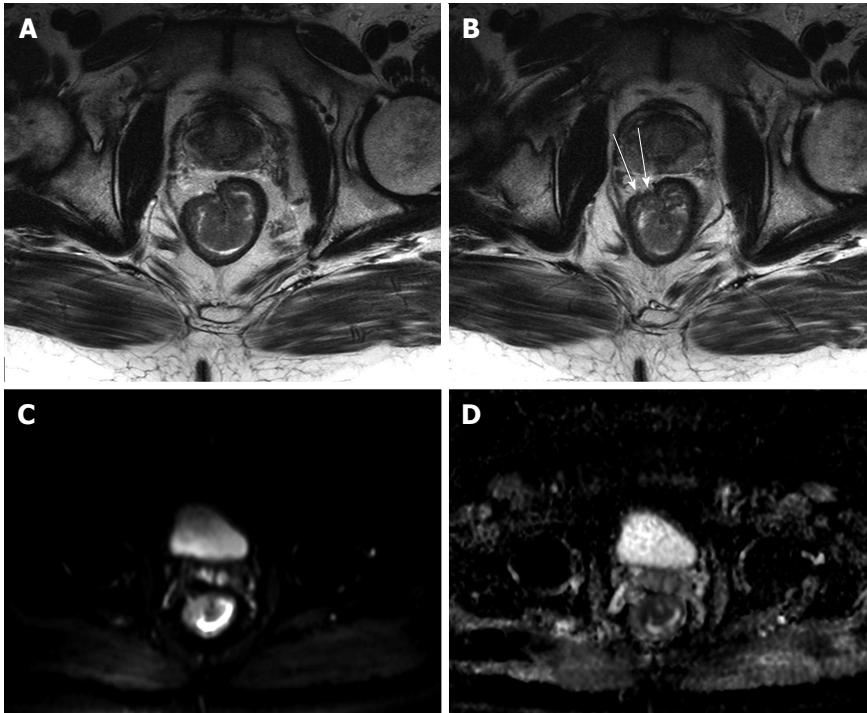


**Figure 28 Stage T3 rectal cancer.** A and B: Axial high-resolution T2-weighted images as well as axial (C) diffusion-weighted imaging ( $b = 650 \text{ s/mm}^2$ ) and (D) ADC map images. There is a large polypoidal mass lesion arising from the right anterolateral lower rectal wall (A and B) with two foci of tumoral extension beyond the low-signal serosal layer (arrows, B) that show diffusion restriction (C and D) in keeping with stage T3 rectal tumor. ADC: Analog-digital conversion.

tal ultrasound has higher reported accuracy in superficial tumors (T1-T2)<sup>[85]</sup>. A limitation of MR is its inability to easily differentiate T2 from early T3 tumors and certainly cannot differentiate between T1 and T2 cancers<sup>[85]</sup>. With the advent of endorectal coils, the T staging accuracy has been reported to be between 70%-90%<sup>[84,86,87]</sup>; however, patient's compliance, limited availability and cost contribute to its less wide application<sup>[85]</sup>. MRI has 92% accuracy in predicting circumferential resection margin when a cutoff point of 1 mm is used<sup>[88]</sup>. Nodal involvement can be evaluated using MRI, which rely on short-axis nodal measurement, signal heterogeneity of the cortex, marginal irregularity, or surrounding fat infiltration. The use of superparamagnetic iron oxide particles appears to be promising<sup>[89]</sup>. Studies also showed that diffusion weighted imaging and perfusion imaging are useful in following-up tumor treatment response including assessing the response to neoadjuvant therapy and determining residual disease or local tumor recurrence<sup>[90-93]</sup>. The main difficulty in assessing the response to chemoradiation is the distinction between fibrosis with and without residual tumor<sup>[94]</sup>. Studies evaluating the ability of MRI after chemoradiation to predict tumor clearance from the mesorectal fascia have shown a high negative predictive value of 100%, at the expense of many false-positives leading to a low positive predictive value (PPV) of 50%-60%<sup>[95]</sup>. Two studies reported a PPV of 83% and 91% and the PPV increased to 94% when > 70% volume downsizing was combined with MR morphological changes<sup>[96,97]</sup>. The detection of very small volumes of disease remains a problem with techniques that only give information on

morphological data. Although 18-Fludeoxyglucose positron emission tomography provides additional functional information, it cannot solve the problem of detection of residual tumor in fibrosis, as shown by a study on the assessment of clearance from the mesorectal fascia<sup>[98]</sup>.

### **Benign lesions of the small and large bowel**

Some lesions have typical features on MR imaging, which is crucial for a correct diagnosis. For instance, hemangiomas are typically strongly hyperintense on T2-weighted MR images; lipomas or tumors with a marked fat content will show high T1 signal intensity that suppresses on fat-suppressed T1-weighted images (Figure 29). However, many other benign neoplasms such as leiomyomas, fibromas and neurogenic tumors may be indistinguishable from other hypervascular lesions on MRE/MRI.

## **CONCLUSION**

The implementation of fast and ultra-fast sequences and dedicated advanced imaging protocols render MRI an excellent tool for GI imaging. State of the art MRI/MRE has rapidly emerged as successful gastrointestinal imaging modality; offering detailed anatomic and morphologic information and also permitting evaluation of extraluminal manifestation and extension of disease. These features have now been shown to alter physician level of confidence and management procedures including medical or surgical approaches.

The lack of ionizing radiation makes MRI the preferred modality in many GI disease processes, especially

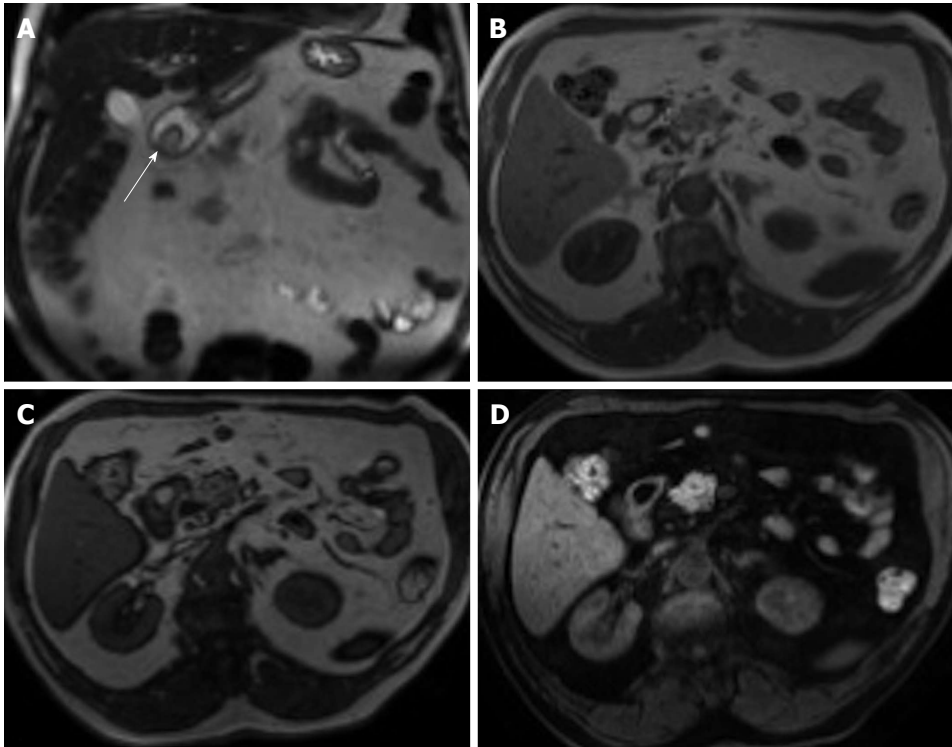


**Figure 29 Duodenal lipoma.** A: Coronal T2-weighted single shot fast spin echo (SSFSE); B: Axial GRE in-phase; C: Opposed-phase T1-weighted; D: Axial fat-suppressed 3D-GRE T1-weighted images. Small, well-defined, intra-luminal, duodenal mass lesion; which demonstrates intermediately high signal on SSFSE (arrow, A), high signal intensity on the in-phase T1 weighted image (B), no drop of signal on the opposed-phase images (C), and homogenously low signal intensity on the fat-suppressed image (D) in keeping with duodenal lipoma. GRE: Gradient recalled echo.

in young patients in the setting of CD, considering that the majority will undergo frequent imaging evaluation. Pregnant patients and those with iodinated contrast agents allergy or decreased renal function may also benefit from MRI. The main drawbacks may be related to relative non-wide availability at present time, economic constrains, and need for highly subspecialized radiologists.

Whenever cross-sectional imaging is requested, especially MRI or CT, the current trend is to weigh the strengths and weaknesses of both techniques considering a risk-benefit analysis. The choice of a diagnostic technique should be determined taking in account patient's age, clinical status and estimated follow-up exams.

## REFERENCES

- 1 **Umschaden HW**, Szolar D, Gasser J, Umschaden M, Haselbach H. Small-bowel disease: comparison of MR enteroclysis images with conventional enteroclysis and surgical findings. *Radiology* 2000; **215**: 717-725 [PMID: 10831690 DOI: 10.1148/radiology.215.3.r00jn12717]
- 2 **Rondonotti E**, Herreras JM, Pennazio M, Caunedo A, Mascarenhas-Saraiva M, de Franchis R. Complications, limitations, and failures of capsule endoscopy: a review of 733 cases. *Gastrointest Endosc* 2005; **62**: 712-716; quiz 752, 754 [PMID: 16246685 DOI: 10.1016/j.gie.2005.05.002]
- 3 **Brenner DJ**, Hall EJ. Computed tomography--an increasing source of radiation exposure. *N Engl J Med* 2007; **357**: 2277-2284 [PMID: 18046031 DOI: 10.1056/NEJMra072149]
- 4 **Froehlich JM**, Patak MA, von Weymarn C, Juli CF, Zollikofer CL, Wentz KU. Small bowel motility assessment with magnetic resonance imaging. *J Magn Reson Imaging* 2005; **21**: 370-375 [PMID: 15779029 DOI: 10.1002/jmri.20284]
- 5 **Cronin CG**, Lohan DG, Browne AM, Roche C, Murphy JM. Does MRI with oral contrast medium allow single-study depiction of inflammatory bowel disease enteritis and colitis? *Eur Radiol* 2010; **20**: 1667-1674 [PMID: 20069426 DOI: 10.1007/s00330-009-1701-2]
- 6 **Ramalho M**, Herédia V, Cardoso C, Matos AP, Palas J, De Freitas J, Semelka RC. Magnetic resonance imaging of small bowel Crohn's disease. *Acta Med Port* 2012; **25**: 231-240 [PMID: 23079251]
- 7 **Lee SS**, Kim AY, Yang SK, Chung JW, Kim SY, Park SH, Ha HK. Crohn disease of the small bowel: comparison of CT enterography, MR enterography, and small-bowel follow-through as diagnostic techniques. *Radiology* 2009; **251**: 751-761 [PMID: 19276325 DOI: 10.1148/radiol.2513081184]
- 8 **Negaard A**, Paulsen V, Sandvik L, Berstad AE, Borthne A, Try K, Lygren I, Storaas T, Klow NE. A prospective randomized comparison between two MRI studies of the small bowel in Crohn's disease, the oral contrast method and MR enteroclysis. *Eur Radiol* 2007; **17**: 2294-2301 [PMID: 17483955 DOI: 10.1007/s00330-007-0648-4]
- 9 **Schreyer AG**, Geissler A, Albrich H, Schölmerich J, Feuerbach S, Rogler G, Völk M, Herfarth H. Abdominal MRI after enteroclysis or with oral contrast in patients with suspected or proven Crohn's disease. *Clin Gastroenterol Hepatol* 2004; **2**: 491-497 [PMID: 15181618]
- 10 **Gupta A**, Postgate AJ, Burling D, Ilangovan R, Marshall M, Phillips RK, Clark SK, Fraser CH. A prospective study of MR enterography versus capsule endoscopy for the surveillance of adult patients with Peutz-Jeghers syndrome. *AJR Am J Roentgenol* 2010; **195**: 108-116 [PMID: 20566803 DOI: 10.2214/AJR.09.3174]
- 11 **Caspari R**, von Falkenhausen M, Krautmacher C, Schild H, Heller J, Sauerbruch T. Comparison of capsule endoscopy and magnetic resonance imaging for the detection of polyps of the small intestine in patients with familial adenomatous polyposis or with Peutz-Jeghers' syndrome. *Endoscopy* 2004;

- 36: 1054-1059 [PMID: 15578294 DOI: 10.1055/s-2004-826041]
- 12 **Kinner S**, Kuehle CA, Herbig S, Haag S, Ladd SC, Barkhausen J, Lauenstein TC. MRI of the small bowel: can sufficient bowel distension be achieved with small volumes of oral contrast? *Eur Radiol* 2008; **18**: 2542-2548 [PMID: 18500525 DOI: 10.1007/s00330-008-1041-7]
  - 13 **Kuehle CA**, Ajaj W, Ladd SC, Massing S, Barkhausen J, Lauenstein TC. Hydro-MRI of the small bowel: effect of contrast volume, timing of contrast administration, and data acquisition on bowel distention. *AJR Am J Roentgenol* 2006; **187**: W375-W385 [PMID: 16985108 DOI: 10.2214/AJR.05.1079]
  - 14 **Laghi A**, Paolantonio P, Iafra F, Borrelli O, Dito L, Tomei E, Cucchiara S, Passariello R. MR of the small bowel with a biphasic oral contrast agent (polyethylene glycol): technical aspects and findings in patients affected by Crohn's disease. *Radiol Med* 2003; **106**: 18-27 [PMID: 12951547]
  - 15 **Ajaj W**, Goehde SC, Schneemann H, Ruehm SG, Debatin JF, Lauenstein TC. Oral contrast agents for small bowel MRI: comparison of different additives to optimize bowel distension. *Eur Radiol* 2004; **14**: 458-464 [PMID: 14634782 DOI: 10.1007/s00330-003-2177-0]
  - 16 **Prassopoulos P**, Papanikolaou N, Grammatikakis J, Rousomoustakaki M, Maris T, Gourtsoyiannis N. MR enteroclysis imaging of Crohn disease. *Radiographics* 2001; **21** Spec No: S161-S172 [PMID: 11598255 DOI: 10.1148/radiographics.21.suppl\_1.g01oc02s161]
  - 17 **Martin DR**, Danrad R, Herrmann K, Semelka RC, Hussain SM. Magnetic resonance imaging of the gastrointestinal tract. *Top Magn Reson Imaging* 2005; **16**: 77-98 [PMID: 16314698]
  - 18 **Kiryu S**, Dodanuki K, Takao H, Watanabe M, Inoue Y, Takazoe M, Sahara R, Unuma K, Ohtomo K. Free-breathing diffusion-weighted imaging for the assessment of inflammatory activity in Crohn's disease. *J Magn Reson Imaging* 2009; **29**: 880-886 [PMID: 19306416 DOI: 10.1002/jmri.21725]
  - 19 **Oto A**, Kayhan A, Williams JT, Fan X, Yun L, Arkani S, Rubin DT. Active Crohn's disease in the small bowel: evaluation by diffusion weighted imaging and quantitative dynamic contrast enhanced MR imaging. *J Magn Reson Imaging* 2011; **33**: 615-624 [PMID: 21563245 DOI: 10.1002/jmri.22435]
  - 20 **Maglente DD**, Gourtsoyiannis N, Rex D, Howard TJ, Kelvin FM. Classification of small bowel Crohn's subtypes based on multimodality imaging. *Radiol Clin North Am* 2003; **41**: 285-303 [PMID: 12659339]
  - 21 **Martin DR**, Kalb B, Sauer CG, Alazraki A, Goldschmid S. Magnetic resonance enterography in Crohn's disease: techniques, interpretation, and utilization for clinical management. *Diagn Interv Radiol* 2012; **18**: 374-386 [PMID: 22517074 DOI: 10.4261/1305-3825.DIR.4893-11.2]
  - 22 **Martin DR**, Lauenstein T, Sitaraman SV. Utility of magnetic resonance imaging in small bowel Crohn's disease. *Gastroenterology* 2007; **133**: 385-390 [PMID: 17681157 DOI: 10.1053/j.gastro.2007.06.036]
  - 23 **Marcos HB**, Semelka RC. Evaluation of Crohn's disease using half-fourier RARE and gadolinium-enhanced SGE sequences: initial results. *Magn Reson Imaging* 2000; **18**: 263-268 [PMID: 10745134]
  - 24 **Albert JG**, Martiny F, Krummenerl A, Stock K, Lesske J, Göbel CM, Lotterer E, Nietsch HH, Behrmann C, Fleig WE. Diagnosis of small bowel Crohn's disease: a prospective comparison of capsule endoscopy with magnetic resonance imaging and fluoroscopic enteroclysis. *Gut* 2005; **54**: 1721-1727 [PMID: 16020490 DOI: 10.1136/gut.2005.069427]
  - 25 **Low RN**, Sebrechts CP, Politoske DA, Bennett MT, Flores S, Snyder RJ, Pressman JH. Crohn disease with endoscopic correlation: single-shot fast spin-echo and gadolinium-enhanced fat-suppressed spoiled gradient-echo MR imaging. *Radiology* 2002; **222**: 652-660 [PMID: 11867781 DOI: 10.1148/radiol.2223010811]
  - 26 **Semelka RC**, Shoenut JP, Silverman R, Kroeker MA, Yaffe CS, Micflikier AB. Bowel disease: prospective comparison of CT and 1.5-T pre- and postcontrast MR imaging with T1-weighted fat-suppressed and breath-hold FLASH sequences. *J Magn Reson Imaging* 1991; **1**: 625-632 [PMID: 1823167]
  - 27 **Low RN**, Francis IR, Politoske D, Bennett M. Crohn's disease evaluation: comparison of contrast-enhanced MR imaging and single-phase helical CT scanning. *J Magn Reson Imaging* 2000; **11**: 127-135 [PMID: 10713944 DOI: 10.1002/(SICI)1522-2586(200002)11:2<127::AID-JMRI8>3.0.CO;2-G]
  - 28 **Masselli G**, Gualdi G. MR imaging of the small bowel. *Radiology* 2012; **264**: 333-348 [PMID: 22821694 DOI: 10.1148/radiol.12111658]
  - 29 **Choi D**, Jin Lee S, Ah Cho Y, Lim HK, Hoon Kim S, Jae Lee W, Hoon Lim J, Park H, Rae Lee Y. Bowel wall thickening in patients with Crohn's disease: CT patterns and correlation with inflammatory activity. *Clin Radiol* 2003; **58**: 68-74 [PMID: 12565208]
  - 30 **Taylor SA**, Punwani S, Rodriguez-Justo M, Bainbridge A, Greenhalgh R, De Vita E, Forbes A, Cohen R, Windsor A, Obichere A, Hansmann A, Rajan J, Novelli M, Halligan S. Mural Crohn disease: correlation of dynamic contrast-enhanced MR imaging findings with angiogenesis and inflammation at histologic examination--pilot study. *Radiology* 2009; **251**: 369-379 [PMID: 19276323 DOI: 10.1148/radiol.2512081292]
  - 31 **Schunk K**, Kern A, Oberholzer K, Kalden P, Mayer I, Orth T, Wanitschke R. Hydro-MRI in Crohn's disease: appraisal of disease activity. *Invest Radiol* 2000; **35**: 431-437 [PMID: 10901105]
  - 32 **Masselli G**, Gualdi G. CT and MR enterography in evaluating small bowel diseases: when to use which modality? *Abdom Imaging* 2013; **38**: 249-259 [PMID: 23011551 DOI: 10.1007/s00261-012-9961-8]
  - 33 **Froehlich JM**, Waldherr C, Stoupis C, Erturk SM, Patak MA. MR motility imaging in Crohn's disease improves lesion detection compared with standard MR imaging. *Eur Radiol* 2010; **20**: 1945-1951 [PMID: 20379822 DOI: 10.1007/s00330-010-1759-x]
  - 34 **Rimola J**, Ordás I, Rodríguez S, Panés J. Colonic Crohn's disease: value of magnetic resonance colonography for detection and quantification of disease activity. *Abdom Imaging* 2010; **35**: 422-427 [PMID: 19536590 DOI: 10.1007/s00261-009-9545-4]
  - 35 **Rimola J**, Ordás I, Rodríguez S, García-Bosch O, Aceituno M, Llach J, Ayuso C, Ricart E, Panés J. Magnetic resonance imaging for evaluation of Crohn's disease: validation of parameters of severity and quantitative index of activity. *Inflamm Bowel Dis* 2011; **17**: 1759-1768 [PMID: 21744431 DOI: 10.1002/ibd.21551]
  - 36 **Rimola J**, Rodríguez S, García-Bosch O, Ordás I, Ayala E, Aceituno M, Pellisé M, Ayuso C, Ricart E, Donoso L, Panés J. Magnetic resonance for assessment of disease activity and severity in ileocolonic Crohn's disease. *Gut* 2009; **58**: 1113-1120 [PMID: 19136510 DOI: 10.1136/gut.2008.167957]
  - 37 **Rimola J**, Ordás I, Rodríguez S, Ricart E, Panés J. Imaging indexes of activity and severity for Crohn's disease: current status and future trends. *Abdom Imaging* 2012; **37**: 958-966 [PMID: 22072290 DOI: 10.1007/s00261-011-9820-z]
  - 38 **Giusti S**, Faggioni L, Neri E, Fruzzetti E, Nardini L, Marchi S, Bartolozzi C. Dynamic MRI of the small bowel: usefulness of quantitative contrast-enhancement parameters and time-signal intensity curves for differentiating between active and inactive Crohn's disease. *Abdom Imaging* 2010; **35**: 646-653 [DOI: 10.1007/s00261-010-9624-6]
  - 39 **Oto A**, Zhu F, Kulkarni K, Karczmar GS, Turner JR, Rubin D. Evaluation of diffusion-weighted MR imaging for detection of bowel inflammation in patients with Crohn's disease. *Acad Radiol* 2009; **16**: 597-603 [PMID: 19282206 DOI: 10.1016/j.acra.2008.11.009]
  - 40 **Ciclitira PJ**, King AL, Fraser JS. AGA technical review on Celiac Sprue. American Gastroenterological Association.

- Gastroenterology* 2001; **120**: 1526-1540 [PMID: 11313324]
- 41 **Paolantonio P**, Tomei E, Rengo M, Ferrari R, Lucchesi P, Laghi A. Adult celiac disease: MRI findings. *Abdom Imaging* 2007; **32**: 433-440 [PMID: 16967239 DOI: 10.1007/s00261-006-9089-9]
  - 42 **Tomei E**, Semelka RC, Braga L, Laghi A, Paolantonio P, Marini M, Passariello R, Di Tola M, Sabbatella L, Picarelli A. Adult celiac disease: what is the role of MRI? *J Magn Reson Imaging* 2006; **24**: 625-629 [PMID: 16888777 DOI: 10.1002/jmri.20664]
  - 43 **AGA Institute**. AGA Institute Medical Position Statement on the Diagnosis and Management of Celiac Disease. *Gastroenterology* 2006; **131**: 1977-1980 [PMID: 17087935 DOI: 10.1053/j.gastro.2006.10.003]
  - 44 **Chott A**, Vesely M, Simonitsch I, Mosberger I, Hanak H. Classification of intestinal T-cell neoplasms and their differential diagnosis. *Am J Clin Pathol* 1999; **111**: S68-S74 [PMID: 9894471]
  - 45 **Lauenstein TC**, Umutlu L, Kloeters C, Aschoff AJ, Ladd ME, Kinner S. Small bowel imaging with MRI. *Acad Radiol* 2012; **19**: 1424-1433 [PMID: 22841341 DOI: 10.1016/j.acra.2012.05.019]
  - 46 **Palmer JA**, Bush RS. Radiation injuries to the bowel associated with the treatment of carcinoma of the cervix. *Surgery* 1976; **80**: 458-464 [PMID: 968730]
  - 47 **Miller DG**, Ivey M, Young J. Home parenteral nutrition in treatment of severe radiation enteritis. *Ann Intern Med* 1979; **91**: 858-860 [PMID: 42336]
  - 48 **Beattie RM**, Croft NM, Fell JM, Afzal NA, Heuschkel RB. Inflammatory bowel disease. *Arch Dis Child* 2006; **91**: 426-432 [PMID: 16632672 DOI: 10.1136/adc.2005.080481]
  - 49 **Loftus EV**. Clinical epidemiology of inflammatory bowel disease: Incidence, prevalence, and environmental influences. *Gastroenterology* 2004; **126**: 1504-1517 [PMID: 15168363]
  - 50 **Gandolfi L**. Comparison of magnetic resonance imaging and endoscopy in distinguishing the type and severity of inflammatory bowel disease. *Gastrointest Endosc* 1996; **43**: 86-87 [PMID: 9026433]
  - 51 **Horsthuis K**, Bipat S, Stokkers PC, Stoker J. Magnetic resonance imaging for evaluation of disease activity in Crohn's disease: a systematic review. *Eur Radiol* 2009; **19**: 1450-1460 [PMID: 19189109 DOI: 10.1007/s00330-008-1287-0]
  - 52 **Heverhagen JT**, Sitter H, Zielke A, Klose KJ. Prospective evaluation of the value of magnetic resonance imaging in suspected acute sigmoid diverticulitis. *Dis Colon Rectum* 2008; **51**: 1810-1815 [PMID: 18443876 DOI: 10.1007/s10350-008-9330-4]
  - 53 **Buckley O**, Geoghegan T, McAuley G, Persaud T, Khosa F, Torreggiani WC. Pictorial review: magnetic resonance imaging of colonic diverticulitis. *Eur Radiol* 2007; **17**: 221-227 [PMID: 16625348 DOI: 10.1007/s00330-006-0236-z]
  - 54 **Destigter KK**, Keating DP. Imaging update: acute colonic diverticulitis. *Clin Colon Rectal Surg* 2009; **22**: 147-155 [PMID: 20676257 DOI: 10.1055/s-0029-1236158]
  - 55 **Hong JJ**, Cohn SM, Ekeh AP, Newman M, Salama M, Leblang SD. A prospective randomized study of clinical assessment versus computed tomography for the diagnosis of acute appendicitis. *Surg Infect (Larchmt)* 2003; **4**: 231-239 [PMID: 14588157 DOI: 10.1089/109629603322419562]
  - 56 **Ralls PW**, Balfe DM, Bree RL, DiSantis DJ, Glick SN, Levine MS, Megibow AJ, Saini S, Shuman WP, Greene FL, Laine LA, Lillemoe K. Evaluation of acute right lower quadrant pain. American College of Radiology. ACR Appropriateness Criteria. *Radiology* 2000; **215** Suppl: 159-166 [PMID: 11037421]
  - 57 **Raman SS**, Osuagwu FC, Kadell B, Cryer H, Sayre J, Lu DS. Effect of CT on false positive diagnosis of appendicitis and perforation. *N Engl J Med* 2008; **358**: 972-973 [PMID: 18305278 DOI: 10.1056/NEJMc0707000]
  - 58 **Daly CP**, Cohan RH, Francis IR, Caoili EM, Ellis JH, Nan B. Incidence of acute appendicitis in patients with equivocal CT findings. *AJR Am J Roentgenol* 2005; **184**: 1813-1820 [PMID: 15908536 DOI: 10.2214/ajr.184.6.01841813]
  - 59 **Pereira JM**, Sirlin CB, Pinto PS, Jeffrey RB, Stella DL, Casola G. Disproportionate fat stranding: a helpful CT sign in patients with acute abdominal pain. *Radiographics* 2004; **24**: 703-715 [PMID: 15143223]
  - 60 **Bixby SD**, Lucey BC, Soto JA, Theysohn JM, Ozonoff A, Varghese JC. Perforated versus nonperforated acute appendicitis: accuracy of multidetector CT detection. *Radiology* 2006; **241**: 780-786 [PMID: 17114626 DOI: 10.1148/radiol.2413051896]
  - 61 **Stoker J**, van Randen A, Laméris W, Boermeester MA. Imaging patients with acute abdominal pain. *Radiology* 2009; **253**: 31-46 [PMID: 19789254 DOI: 10.1148/radiol.2531090302]
  - 62 **Wallace GW**, Davis MA, Semelka RC, Fielding JR. Imaging the pregnant patient with abdominal pain. *Abdom Imaging* 2012; **37**: 849-860 [PMID: 22160283 DOI: 10.1007/s00261-011-9827-5]
  - 63 **Leeuwenburgh MM**, Wiarda BM, Wiezer MJ, Vrouwenraets BC, Gratama JW, Spilt A, Richir MC, Bossuyt PM, Stoker J, Boermeester MA. Comparison of imaging strategies with conditional contrast-enhanced CT and unenhanced MR imaging in patients suspected of having appendicitis: a multicenter diagnostic performance study. *Radiology* 2013; **268**: 135-143 [PMID: 23481162 DOI: 10.1148/radiol.13121753]
  - 64 **Leeuwenburgh MM**, Jensch S, Gratama JW, Spilt A, Wiarda BM, Van Es HW, Cobben LP, Bossuyt PM, Boermeester MA, Stoker J. MRI features associated with acute appendicitis. *Eur Radiol* 2014; **24**: 214-222 [PMID: 24013847 DOI: 10.1007/s00330-013-3001-0]
  - 65 **Borrmann R**. Geschwulste des Magens und des Duodenum. In: Henke F, Lubarsch O. Handbuch der speziellen pathologischen Anatomie und Histologie. Berlin: Verlag von J Springer, 1926: 812-1054
  - 66 **Marcos HB**, Semelka RC. Stomach diseases: MR evaluation using combined t2-weighted single-shot echo train spin-echo and gadolinium-enhanced spoiled gradient-echo sequences. *J Magn Reson Imaging* 1999; **10**: 950-960 [PMID: 10581508 DOI: 10.1002/(SICI)1522-2586(199912)10:6<950::AID-JMRI7>3.0.CO;2-H]
  - 67 **Maccioni F**, Marcelli G, Al Ansari N, Zippi M, De Marco V, Kagarmanova A, Vestri A, Marcheggiano-Clarke L, Marini M. Preoperative T and N staging of gastric cancer: magnetic resonance imaging (MRI) versus multi detector computed tomography (MDCT). *Clin Ter* 2010; **161**: e57-e62 [PMID: 20499021]
  - 68 **Sohn KM**, Lee JM, Lee SY, Ahn BY, Park SM, Kim KM. Comparing MR imaging and CT in the staging of gastric carcinoma. *AJR Am J Roentgenol* 2000; **174**: 1551-1557 [PMID: 10845479 DOI: 10.2214/ajr.174.6.1741551]
  - 69 **Miettinen M**, Lasota J. Gastrointestinal stromal tumors--definition, clinical, histological, immunohistochemical, and molecular genetic features and differential diagnosis. *Virchows Arch* 2001; **438**: 1-12 [PMID: 11213830]
  - 70 **Chourmouzi D**, Sinakos E, Papalavrentios L, Akriviadis E, Drevelegas A. Gastrointestinal stromal tumors: a pictorial review. *J Gastrointest Liver Dis* 2009; **18**: 379-383 [PMID: 19795038]
  - 71 **Stroszczyński C**, Jost D, Reichardt P, Chmelik P, Gaffke G, Kretzschmar A, Schneider U, Felix R, Hohenberger P. Follow-up of gastro-intestinal stromal tumours (GIST) during treatment with imatinib mesylate by abdominal MRI. *Eur Radiol* 2005; **15**: 2448-2456 [PMID: 16132930 DOI: 10.1007/s00330-005-2867-x]
  - 72 **Ghimire P**, Wu GY, Zhu L. Primary gastrointestinal lymphoma. *World J Gastroenterol* 2011; **17**: 697-707 [PMID: 21390139 DOI: 10.3748/wjg.v17.i6.697]
  - 73 **Masselli G**, Colaiacomo MC, Marcelli G, Bertini L, Casciani E, Laghi F, D'Amico P, Caprasecca S, Poletti E, Gualdi G. MRI of the small-bowel: how to differentiate primary neo-

- plasms and mimickers. *Br J Radiol* 2012; **85**: 824-837 [PMID: 22422388 DOI: 10.1259/bjr/14517468]
- 74 **Masselli G**, Gualdi G. Evaluation of small bowel tumors: MR enteroclysis. *Abdom Imaging* 2010; **35**: 23-30 [PMID: 19096749 DOI: 10.1007/s00261-008-9490-7]
- 75 **Minardi AJ**, Zibari GB, Aultman DF, McMillan RW, McDonald JC. Small-bowel tumors. *J Am Coll Surg* 1998; **186**: 664-668 [PMID: 9632155]
- 76 **Amzallag-Bellenger E**, Oudjit A, Ruiz A, Cadot G, Soyer PA, Hoeffel CC. Effectiveness of MR enterography for the assessment of small-bowel diseases beyond Crohn disease. *Radiographics* 2012; **32**: 1423-1444 [PMID: 22977028 DOI: 10.1148/rg.325115088]
- 77 **Hoeffel C**, Crema MD, Belkacem A, Azizi L, Lewin M, Arrivé L, Tubiana JM. Multi-detector row CT: spectrum of diseases involving the ileocecal area. *Radiographics* 2006; **26**: 1373-1390 [PMID: 16973770 DOI: 10.1148/rg.265045191]
- 78 **Beaumont C**, Pandey T, Gaines Fricke R, Laryea J, Jambhekar K. MR evaluation of rectal cancer: current concepts. *Curr Probl Diagn Radiol* 2013; **42**: 99-112 [PMID: 23683851 DOI: 10.1067/j.cpradiol.2012.08.002]
- 79 **Shoenut JP**, Semelka RC, Silverman R, Yaffe CS, Micflikier AB. Magnetic resonance imaging evaluation of the local extent of colorectal mass lesions. *J Clin Gastroenterol* 1993; **17**: 248-253 [PMID: 8228088]
- 80 **Zijta FM**, Bipat S, Stoker J. Magnetic resonance (MR) colonography in the detection of colorectal lesions: a systematic review of prospective studies. *Eur Radiol* 2010; **20**: 1031-1046 [PMID: 19936754 DOI: 10.1007/s00330-009-1663-4]
- 81 **Taylor FG**, Swift RI, Blomqvist L, Brown G. A systematic approach to the interpretation of preoperative staging MRI for rectal cancer. *AJR Am J Roentgenol* 2008; **191**: 1827-1835 [PMID: 19020255 DOI: 10.2214/AJR.08.1004]
- 82 **Karatağ O**, Karatağ GY, Özkurt H, Değirmenci HK, Avlanmış Ö, Başak M, Baykan A. The ability of phased-array MRI in preoperative staging of primary rectal cancer: correlation with histopathological results. *Diagn Interv Radiol* 2012; **18**: 20-26 [PMID: 21671218 DOI: 10.4261/1305-3825.DIR.3394-10.2]
- 83 **Halefoglu AM**, Yildirim S, Avlanmis O, Sakiz D, Baykan A. Endorectal ultrasonography versus phased-array magnetic resonance imaging for preoperative staging of rectal cancer. *World J Gastroenterol* 2008; **14**: 3504-3510 [PMID: 18567078]
- 84 **MERCURY Study Group**. Diagnostic accuracy of preoperative magnetic resonance imaging in predicting curative resection of rectal cancer: prospective observational study. *BMJ* 2006; **333**: 779 [PMID: 16984925 DOI: 10.1136/bmj.38937.646400.55]
- 85 **Samee A**, Selvasekar CR. Current trends in staging rectal cancer. *World J Gastroenterol* 2011; **17**: 828-834 [PMID: 21412492 DOI: 10.3748/wjg.v17.i7.828]
- 86 **Beets-Tan RG**, Beets GL, Vliegen RF, Kessels AG, Van Boven H, De Bruine A, von Meyenfeldt MF, Baeten CG, van Engelshoven JM. Accuracy of magnetic resonance imaging in prediction of tumour-free resection margin in rectal cancer surgery. *Lancet* 2001; **357**: 497-504 [PMID: 11229667]
- 87 **Hünerbein M**, Pegios W, Rau B, Vogl TJ, Felix R, Schlag PM. Prospective comparison of endorectal ultrasound, three-dimensional endorectal ultrasound, and endorectal MRI in the preoperative evaluation of rectal tumors. Preliminary results. *Surg Endosc* 2000; **14**: 1005-1009 [PMID: 11116406 DOI: 10.1007/s004640000345]
- 88 **Brown G**, Radcliffe AG, Newcombe RG, Dallimore NS, Bourne MW, Williams GT. Preoperative assessment of prognostic factors in rectal cancer using high-resolution magnetic resonance imaging. *Br J Surg* 2003; **90**: 355-364 [PMID: 12594673 DOI: 10.1002/bjs.4034]
- 89 **Koh DM**, Brown G, Temple L, Raja A, Toomey P, Bett N, Norman AR, Husband JE. Rectal cancer: mesorectal lymph nodes at MR imaging with USPIO versus histopathologic findings--initial observations. *Radiology* 2004; **231**: 91-99 [PMID: 14976266]
- 90 **Park MJ**, Kim SH, Lee SJ, Jang KM, Rhim H. Locally advanced rectal cancer: added value of diffusion-weighted MR imaging for predicting tumor clearance of the mesorectal fascia after neoadjuvant chemotherapy and radiation therapy. *Radiology* 2011; **260**: 771-780 [PMID: 21846762 DOI: 10.1148/radiol.111102135]
- 91 **Gollub MJ**, Gultekin DH, Akin O, Do RK, Fuqua JL, Gonen M, Kuk D, Weiser M, Saltz L, Schrag D, Goodman K, Paty P, Guillem J, Nash GM, Temple L, Shia J, Schwartz LH. Dynamic contrast enhanced-MRI for the detection of pathological complete response to neoadjuvant chemotherapy for locally advanced rectal cancer. *Eur Radiol* 2012; **22**: 821-831 [PMID: 22101743 DOI: 10.1007/s00330-011-2321-1]
- 92 **Lambregts DM**, Cappendijk VC, Maas M, Beets GL, Beets-Tan RG. Value of MRI and diffusion-weighted MRI for the diagnosis of locally recurrent rectal cancer. *Eur Radiol* 2011; **21**: 1250-1258 [PMID: 21240647 DOI: 10.1007/s00330-010-2052-8]
- 93 **Sassen S**, de Booi M, Sosef M, Berendsen R, Lammering G, Clarijs R, Bakker M, Beets-Tan R, Warmerdam F, Vliegen R. Locally advanced rectal cancer: is diffusion weighted MRI helpful for the identification of complete responders (ypT0N0) after neoadjuvant chemoradiation therapy? *Eur Radiol* 2013; **23**: 3440-3449 [PMID: 23832319 DOI: 10.1007/s00330-013-2956-1]
- 94 **Beets-Tan RG**, Beets GL. Local staging of rectal cancer: a review of imaging. *J Magn Reson Imaging* 2011; **33**: 1012-1019 [PMID: 21509856 DOI: 10.1002/jmri.22475]
- 95 **Chen CC**, Lee RC, Lin JK, Wang LW, Yang SH. How accurate is magnetic resonance imaging in restaging rectal cancer in patients receiving preoperative combined chemoradiotherapy? *Dis Colon Rectum* 2005; **48**: 722-728 [PMID: 15747073 DOI: 10.1007/s10350-004-0851-1]
- 96 **Dresen RC**, Beets GL, Rutten HJ, Engelen SM, Lahaye MJ, Vliegen RF, de Bruine AP, Kessels AG, Lammering G, Beets-Tan RG. Locally advanced rectal cancer: MR imaging for restaging after neoadjuvant radiation therapy with concomitant chemotherapy. Part I. Are we able to predict tumor confined to the rectal wall? *Radiology* 2009; **252**: 71-80 [PMID: 19403847 DOI: 10.1148/radiol.2521081200]
- 97 **Barbaro B**, Fiorucci C, Tebala C, Valentini V, Gambacorta MA, Vecchio FM, Rizzo G, Coco C, Crucitti A, Ratto C, Bonomo L. Locally advanced rectal cancer: MR imaging in prediction of response after preoperative chemotherapy and radiation therapy. *Radiology* 2009; **250**: 730-739 [PMID: 19244043 DOI: 10.1148/radiol.2503080310]
- 98 **Vliegen RF**, Beets GL, Lammering G, Dresen RC, Rutten HJ, Kessels AG, Oei TK, de Bruine AP, van Engelshoven JM, Beets-Tan RG. Mesorectal fascia invasion after neoadjuvant chemotherapy and radiation therapy for locally advanced rectal cancer: accuracy of MR imaging for prediction. *Radiology* 2008; **246**: 454-462 [PMID: 18227541 DOI: 10.1148/radiol.2462070042]

**P- Reviewer:** Chen F, Imbriaco M, Lichtor T **S- Editor:** Ji FF  
**L- Editor:** A **E- Editor:** Liu SQ





Published by **Baishideng Publishing Group Inc**

8226 Regency Drive, Pleasanton, CA 94588, USA

Telephone: +1-925-223-8242

Fax: +1-925-223-8243

E-mail: [bpgoffice@wjgnet.com](mailto:bpgoffice@wjgnet.com)

Help Desk: <http://www.wjgnet.com/esps/helpdesk.aspx>

<http://www.wjgnet.com>

